Treb. Mus. Geol. Barcelona, 11: 5-65 (2002)

The mid-Tertiary Azuara and Rubielos de la Cérida paired impact structures (Spain)*

Kord ERNSTSON**, Fernando CLAUDIN***, Ulrich SCHÜSSLER**** and Klaudia HRADIL****

RESUMEN

ERNSTSON, K., CLAUDIN, F., SCHÜSSLER, U. and HRADIL, K. Las estructuras de impacto doble del terciario medio de Azuara y Rubielos de la Cérida (España).

El presente artículo se centra en las estructuras de impacto de Azuara y Rubielos de la Cérida, que con diámetros de aproximadamente 35-40 Km fueron generadas en un objetivo puramente sedimentario. Ambas constituyen la estructura terrestre de impacto doble de mayor tamaño conocida hasta el momento. A partir de los datos estratigráficos y paleontológicos, su edad más probable es Eoceno sup. u Oligoceno. La cartografia geológica realizada ha permitido localizar abundantes evidencias de impacto e incluso efectos del impacto en depósitos autóctonos distantes. La evidencia de impacto más importante para ambas estructuras viene dada por la presencia de un intenso metamorfismo de choque, incluyendo fundido y vidrio diapléctico, rasgos de deformación planar (PDFs), diferentes tipos de rocas de fundido de impacto (formadas a partir de fundido silicatado, de fundido carbonatado y fundido de carbonato-fosfato) y brechas suevíticas. Partículas de vidrio carbonoso amorfo sitas en un componente sólido de C-O pueden estar relacionadas con fullerenos, y haberse formado a partir del enfriamiento de un fundido procedente o bien de carbón intensamente chocado o bien de calizas intensamente chocadas. Pensamos que el impacto tuvo una influencia considerable en el terciario medio de esta región del Sistema Ibérico, y sugerimos que aquellos modelos en los que no se ha tenido en cuenta este evento peculiar y de amplia repercusión necesitan una revisión considerable.

Palabras clave: Estructura de impacto de Azuara, estructura de impacto de rubielos de la Cérida, Cadena Ibérica (España), metamorfismo de choque, rocas de fundido de impacto, brechas de impacto, eyecta, Terciario.

---

* Dr. Francisco Anguita, Associate Professor (Planetary Geology), Universidad Complutense de Madrid (Spain), referee of this work, sent us the following remarks:
"In my opinion, the present paper means a quantic jump towards the confirmation of Azuara and Rubielos de la Cérida structures as a doublet impact crater. Specifically, the analyses performed at centimeter to microscopic scales, reveal a body of evidence difficult to contradict. Any future research on this area will have to discuss necessarily the interpretations now offered by Ernstson *et al.* Lacking this discussion, any hypothesis defending that Azuara and Rubielos structures are the result of "normal" sedimentary and tectonic processes will be utterly untenable."

** Fakultät für Geowissenschaften der Universität Würzburg, Pleicherwall 1, D-97070 Würzburg, Germany. www.impact-structures.com
*** IES Giola, Llinars del Vallès. Barcelona-08450, Spain. www.impact-structures.com
**** Institut für Mineralogie der Universität Würzburg, Am Hubland, D-97074 Würzburg, Germany.

ABSTRACT

We report on the Azuara impact structure and its Rubielos de la Cérida companion crater, which establish the largest terrestrial doublet impact structure presently known. Both structures have diameters of roughly 35 – 40 km and they have been formed in a purely sedimentary target. From stratigraphic considerations and palaeontologic dating, an Upper Eocene or Oligocene age is very probable Geological mapping has established abundant geologic impact evidence in the form of monomictic and polymictic breccias and breccia dikes, megabreccias, dislocated megablocks, remarkable structural features, extensive impact ejecta and impact signatures even in distant autochthonous deposits. The most striking impact evidence for both structures is given by strong shock metamorphism, including melt and diaplectic glass, planar deformation features (PDFs), different kinds of impact melt rocks (from former silicate melt, carbonate melt, carbonate-phosphate melt) and suevite breccias. Glassy amorphous carbon particles in a solid C-O compound may be related with fullerenes and may originate from a quenched melt of extremely shocked coal or from extremely shocked limestones. It is assumed that the impact had considerable influence on the Mid-Tertiary regional geology of the Iberian System, and we suggest that respective geologic models which have so far not considered this peculiar and far-reaching event, need considerable revision.

Key words: Azuara impact structure, Rubielos de la Cérida impact structure, Iberian chain (Spain), shock metamorphism, impact melt rocks, impact breccias, ejecta, Tertiary.

INTRODUCTION

Ernstson *et al.* (1985) published the hypothesis of the impact origin for the Azuara structure some 50 km south of Zaragoza (41°10'N, 0°55'W – Fig.1) in 1985. The Azuara impact structure was included in the Earth Impact Database, which was first assembled by researchers of the Geological Survey of Canada in the same year. The Crater Inventory was recently updated and lists 163 proven terrestrial impact structures (http://www.unb.ca/passc/ImpactDatabase/index.html).

Originally, the case for formation of the Azuara structure by impact was based mainly on the occurrence of shock metamorphism (French and Short, 1968; Stöffler, 1972; and others) in polymictic (mixed) breccias. Later, the case for an impact origin was strengthened by geophysical measurements (Ernstson *et al.*, 1987; Ernstson and Fiebag, 1992) and by the detection of extended impact ejecta deposits (Ernstson and Claudín, 1990). Detailed mapping, extensive structural investigations, photogeology and petrographic analyses (Bärle, 1988; Fiebag, 1988; Gwosdek, 1988; König, 1988; Linneweber, 1988; Waasmaier, 1988; Hunoltstein-Bunjevac, 1989; Müller, 1989; Katschorek, 1990; Mayer, 1991; Müller and Ernstson, 1990; Ernstson and Fiebag, 1992; Ernstson, 1994; Feld, pers. comm.) provided a host of impact-related findings and observations. Despite the clear shock metamorphism, the impact evidence is questioned by some regional geologists (Aurell *et al.*, 1993; Aurell, 1994; Cortés *et al.*, 2002), who still claim an endogenetic origin for most of the impact features.

The idea that the impact event not only produced the Azuara structure but also the Rubielos de la Cérida structure, a twin crater of comparable size about 50 km to the south (Fig.1), was first suggested by Ernstson *et al.* (1994) on the basis of the occurrence of strongly deformed Buntsandstein conglomerates peripheral to the Azuara structure (Ernstson *et al.*, 2001a). Since 1994, field work, petrographic and geochemical analyses have shown (Hradil *et al.*, 2001; Claudin *et al.*, 2001; Ernstson *et al.*, 2001b, c) that this Rubielos de la Cérida structure bears all evidence of an impact structure. Stratigraphic considerations suggest Rubielos de la Cérida to be a companion to Azuara and thus we have established that a large doublet impact structure exists in east-central Spain.

Here, we report on the current state of investigations of this doublet impact structure. Most of the data for the Azuara structure have been published previously or can be found in the many diploma theses referred to above. Therefore, this report widely summarizes the comparative results of both the Rubielos de la Cérida and the Azuara structures, with some emphasis focused on new results for Rubielos de la Cérida and on the special situation of a paired impact.

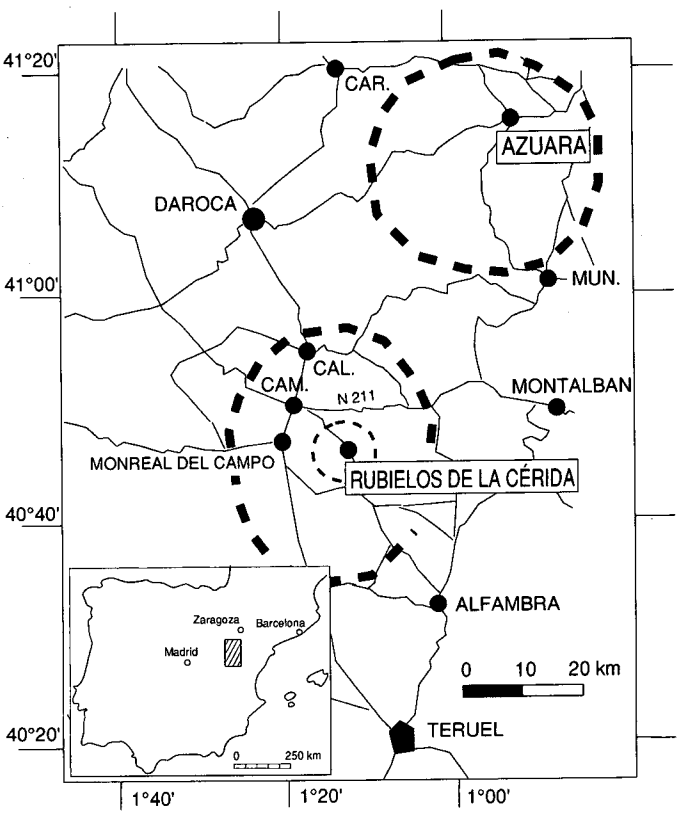

Fig. 1. Location map for the Azuara and Rubielos de la Cérida impact structures. CAL = Calomocha, CAM = Caminreal, CAR = Cariñena, MUN = Muniesa.

Fig 1. Mapa de situación de las estructuras de impacto de Azuara y Rubielos de la Cérida. CAL = Calamocha, CAM = Caminreal, CAR = Cariñena, MUN = Muniesa

THE AZUARA IMPACT STRUCTURE

Topographic features and target rocks

Compared with other large impact structures (e.g., Manicouagan, Ries, Clearwater West), the Azuara structure does not show a particularly striking morphology. Located at the margin between the Alpidic fold belt of the Iberian Chains and the Tertiary Ebro Basin, the structure is characterized by Mesozoic layers emerging from the Ebro Basin Tertiary sediments and forming a ring-like pattern (Fig.2). The diameter of the ring is about 30 km, while the total diameter of the structure is estimated between 35 and 40 km.

The impact affected both the Palaeozoic and the Mesozoic of the Eastern Iberian (the "rama aragonesa") Chain. The Lower Tertiary at the time of the impact is assumed to have been thick (1000 - 2000 m or even more) and predominantly unconsolidated molasse sediments overlaying the Palaeozoic and Mesozoic stable core (Ernstson and Fiebag, 1992). This sedimentary pile has a thickness of more than 10 km (Carls, 1983; Carls and Monninger, 1974) (Fig.3), which shows that despite the large diameter, the Azuara structure was imprinted on a purely sedimentary target (see Grieve and Robertson, 1979; Grieve, 1982), if we neglect a few igneous intercalations of very small dimensions. The dominantly soft target and the advanced erosion may be the cause of the weak morphological signature of the structure.

Impact-geologic features

Breccias

As has been stated previously (Ernstson *et al.*, 1985; Ernstson and Fiebag, 1992), polymictic (mixed) and monomictic (monolithologic) breccias are very abundant throughout the Azuara structure and have been mapped in detail mostly on 1 : 10.000 and 1 : 20.000 scales (Bärle, 1988; Fiebag, 1988; Gwosdek, 1988; König, 1988; Linneweber, 1988; Waasmaier, 1988; Hunoltstein-Bunjevac, 1989; Müller, 1989; Katschorek 1990; Mayer, 1991; Feld, pers. comm.).

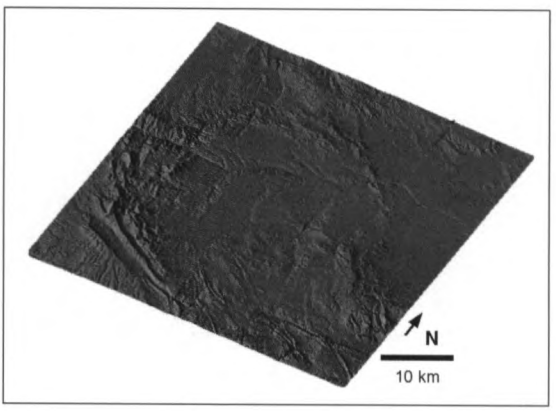

Fig. 2. Morphological signature of the Azuara structure taken from the digital map of Spain, 1 : 250.000. The image has been performed by Manuel Cabedo.

Fig. 2. Imagen morfológica de la estructura de Azuara obtenida a partir del mapa digital de España, 1: 250.000. La imagen fue elaborada por Manuel Cabedo

Basal breccia (suevite breccia)

The original name "basal breccia" (Ernstson and Fiebag, 1992) refers to the fact that this peculiar breccia is regularly found at the base of the post-impact (and post-Alpidic), tectonically undisturbed Upper Tertiary. The up to 20 m thick horizontally bedded breccia layer is always unconformably overlying the folded rocks and at the contacts more or less meshed with them without any re-working or soil formation. Palaeozoic and Mesozoic rocks contribute to the sharp-edged (sometimes subrounded) clasts and minute splinters in an extremely hard and exceptionally cemented carbonate matrix (Pl. 1, Fig. 1) that often displays distinct flow texture. Clasts that are themselves breccias (breccias-within-breccias) are abundant. Frequently, limestone and dolomite clasts show a skeletal and vesicular texture, sometimes to the extent that only the rim of a clast remains and the hollow may contain a residual white powder. High-temperature decarbonization, the formation of carbonate melt and subsequent recombination are the probable causes (Mayer, 1991; Ernstson and Fiebag, 1992; for a comprehensive discussion of the basal breccia and the related carbonate melt see Katschorek [1990]).

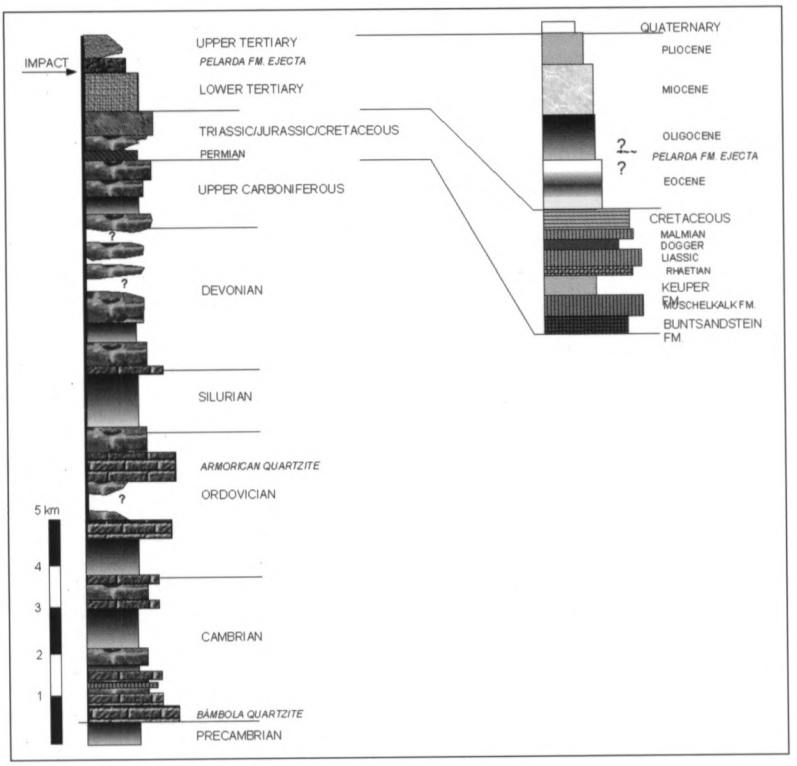

Fig. 3. Stratigraphy of the target rocks in the Iberian chain. Data from Carls and Monninger (1974) and ITGE (1991).

Fig. 3. Estratigrafia de las rocas objetivo en la cadena Ibérica. Datos extraidos de Carls y Monninger (1974) e ITGE (1991)

From X-ray fluorescence and X-ray diffraction analyses and thin-section inspection, Mayer (1991) infers an SiO_2 amorphous phase (up to about 10%) contributing to the matrix. This phase is assumed to be finely dispersed glass. In a few cases, glass particles in the basal breccia can be observed by the optical microscope. Shock-metamorphic effects are frequently observed in minerals from silicate fragments. Most significant is the abundant occurrence of diaplectic quartz in the basal breccia (Mayer, 1991, p.215). The formation of diaplectic quartz requires shock pressures in excess of 15 GPa (= 150 kbar) (Bunch *et al.*, 1968). Planar deformation features (PDFs) are rare, but multiple sets of planar fractures (PFs, cleavage; see Fig. 139 in Fiebag, 1988) in quartz, microtwinning in calcite (Metzler *et al.*, 1988; and references therein) and strong kinkbanding in mica (Hörz, 1970) indicate moderate shock metamorphism. More evidence of shock metamorphism in the Azuara structure is given below. According to the current classification and nomenclature of impact rocks (IUGS Subcommission on the Systematics of Metamorphic Rocks, Study Group for Impactites), this polymictic basal breccia containing shocked clasts and melt, is termed a suevite or suevite breccia.

In Fig.4, basal breccia exposures so far mapped are plotted to show the general distribution, and the following locations are given by their UTM coordinates:

6 70 500, 45 74 700; 6 82 700, 45 75 100; 8 14 350, 7 41 800; 8 15 850, 7 42 650; 6 63 650, 45 73 200; 6 62 350, 45 73 450; 6 65 700, 45 76 500; 6 68 200, 45 76 100; 6 69 600, 45 74 850; 6 75 800, 45 50 600. In the village of Moyuela, the basal breccia has been used as building stone for the construction of a large retaining wall.

Breccia dikes (dike breccias)

Breccia dikes are prominent features in impact structures (Lambert, 1981; Wilshire *et al.*, 1972; Pohl *et al.*, 1977; Dressler, 1970, 1984; Bischoff and Oskierski, 1987, 1988; Schwarzmann *et al.*, 1983; and others). Most researchers believe that they form in the excavation stage of impact cratering (Melosh, 1989) by the injection of material into the floor and the walls of the growing and changing excavation cavity. The Azuara structure presents a large variety of impact breccia dikes (Fiebag, 1988; Ernstson and Fiebag, 1992). They have been mapped in and around the structure in nearly all stratigraphical units, and they have formed independently of the host rock both in silicate and carbonate rocks (Pl. 1, Fig. 2, 3). They are up to 2 m wide and may be traced over a distance of more than 200 m (Mayer, 1991). Whole systems or networks of breccia dikes are developed (see, e.g., Fig. 17 in Ernstson and Fiebag, 1992). An H-type (our definition) breccia-dike system is often observed and characterized by a tying of vertical and horizontal dikes (Pl. 1, Fig. 2). The system is suggested to have formed in a short-term sequence of compressive and tensile stress.

The breccias of the dikes are monomictic and polymictic; two or more breccia generations are frequent. Thereby, breccia dikes may run within or intersect another dike. Often, the breccias do not differ from the basal breccia, and they show the same composition and texture discussed before. Shock metamorphism in the dike breccias is abundant and especially strong in the dikes that have formed in the Palaeozoic target rocks (see below).

Fig.5 shows the locations where prominent breccia dikes and breccia-dike systems are exposed. Apart from the dikes in Pl. 1, Fig. 2, 3, the UTM coordinates are given for locations where breccia dikes can be readily studied: 6 85 380, 45 47 630; 6 88 070, 45 52 540; 6 83 500, 45 75 900; 6 68 035, 45 40 450.

Impact breccia near Almonacid de la Cuba

A peculiar impact breccia is exposed near Almonacid de la Cuba at the NE rim of the structure (Fig. 4; UTM coordinates 6 84 300, 45 73 900) and is so far unique with respect to composition and texture (Pl. 1, Fig. 4). Within a dense to porous and even foamy greyish carbonate matrix, components of snow-white colour are embedded, which are in many cases extremely vesicular. The breccia is part of an extensive

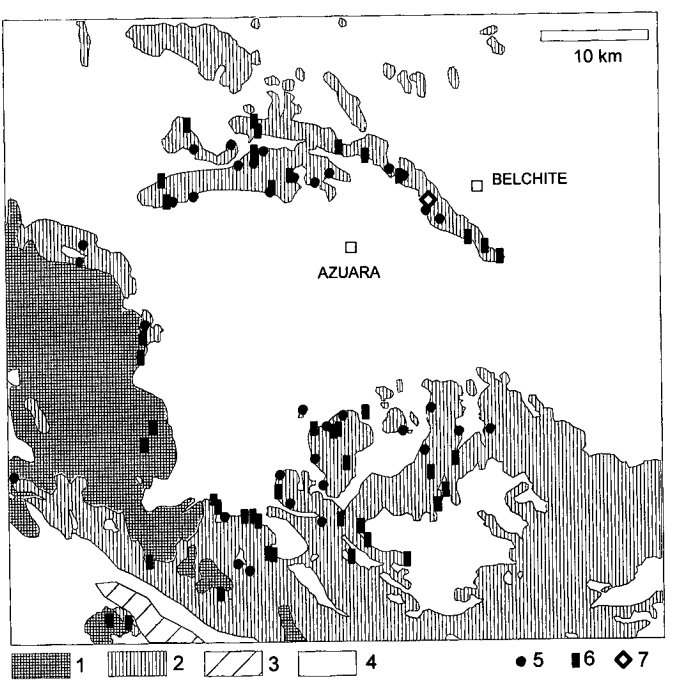

Fig. 4. Location map for impact breccias and breccia dikes in the Azuara structure. Geological sketch map simplified and modified from IGME (1970, 1981) and ITGE (1991). 1 = Palaeozoic, 2 = Mesozoic, 3 = Pelarda Fm. ejecta, 4 = Cenozoic; 5 = basal (suevite) breccia, 6 = breccia dikes, 7 = impact breccia near Almonacid de la Cuba.

Fig. 4. Mapa de situación de los afloramientos de brechas de impacto y diques de brecha en la estructura de Azuara. El mapa geológico ha sido obtenido por simplificación y modificación de los mapas del IGME (1970, 1981) e ITGE (1991). 1 = Paleozoico, 2 = Mesozoico, 3 = eyecta de la Fm. Pelarda, 4 = Cenozoico, 5 = brecha basal (suevita), 6 = diques de brechas, 7 = brecha de impacto cercana a Almonacid de la Cuba

deposit which has been investigated in detail and described by Katschorek (1990). From field work and petrographic analyses, she concludes that the deposit has resulted from an expanded, turbulent, and dilute flow by inclusion of carbonate melt, similar to volcanic surges.

Megabreccia

In the impact literature, extensive breccias consisting of very large components are generally termed megabreccias. Megabreccias have been reported for other impact structures such as Wells Creek, Steinheim basin, Gosses Bluff, Sierra Madera, Wetumpka, and others.

In the Azuara impact structure, the megabreccia in the narrow sense (megabreccias in the broader sense are discussed with the Rubielos de la Cérida structure) is exposed near Belchite/Almonacid de la Cuba and Herrera de los Navarros in the outer ring (Fig. 5). According to the detailed description by Fiebag (1988) and Katschorek (1990), the deposits cover an area of roughly 3 Km^2, their thickness may exceed 80 m, and the largest components have a size up to about 20 m (Pl. 1, Fig. 5). Although

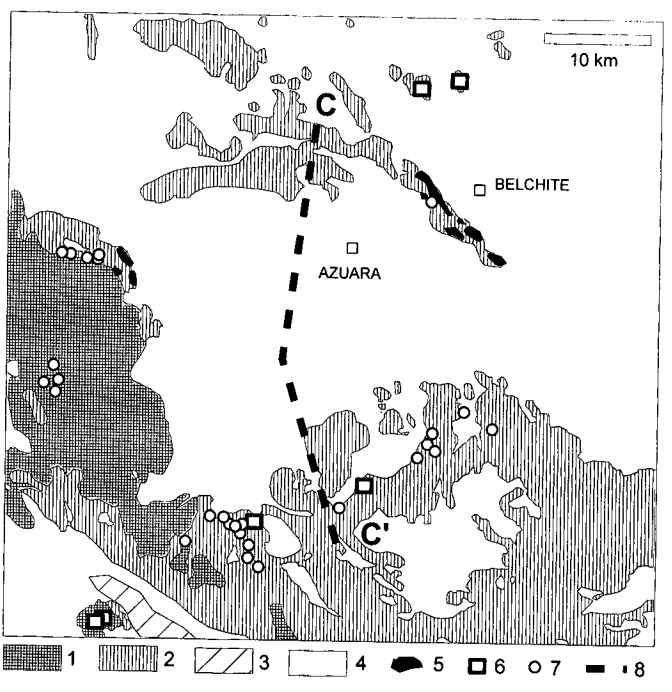

Fig. 5. Location map for the megabreccia (5), monomictic movement breccias (6), dislocated megablocks (7), and the gravity profile in Fig. 6 (8). Geology same as in Fig. 4.

Fig. 5. Mapa de localización de la megabrecha (5), brechas monomícticas de movimiento (6), megabloques dislocados (7), y el perfil de gravedad de la Fig. 6 (8). La geología es la misma que la de la Fig. 4.

the breccia occurs as a nearly stratiform layer by in situ brecciation of Upper Triassic and Liassic limestones (Rhaetian, Hettangian, Sinemurian), it is basically polymictic indicated by the intercalation of allochthonous blocks. Mortar texture and breccia generations (breccias-within-breccias) are abundant, and in thin section, cataclastic flow texture of the matrix is observed.

It is suggested that the megabreccia formed in the beginning modification stage of the impact cratering process by the simultaneous action of the yet ongoing excavation flow and the collapse/rebound of the transient crater (Fiebag, 1988; Katschorek, 1990; Ernstson and Fiebag, 1992). Although the megabreccia partly incorporates the well-known collapse breccias of the Cortes de Tajuña Formation (Goy *et al.*, 1976), a clear distinction should be made (see, e.g., Aurell *et al.* 1992, 1993; Aurell, 1994; Cortés, 1994).

Monomictic movement breccias

The term "monomict movement breccia" has been introduced by Reiff (1978) by discussing monomictic breccia complexes in the Steinheim, Ries, Sierra Madera, Flynn Creek, Decaturville and Wells Creek impact structures. In the Wells Creek impact structure, these breccias were called crackle breccias and homogeneous rubble breccias (Wilson and Stearns, 1968) and later considered variants of the same phenomenon (Reiff 1978). Related textures are grit brecciation and mortar texture (Hüttner, 1969). In each case, a drastic brecciation of whole rock complexes with resulting grain sizes down to sand and silt fraction and frequently preserved fitting of the fragments is observed. This peculiar brecciation requires intense movement under very high confining pressure. In the impact structures referred to above, these movement breccias occur in excavated/ejected megablocks, in the crater floor, in inner rings and central uplifts. Reiff (1978) points to the fact that the typical texture of monomictic movement breccias is also observed in breccias from giant rock falls (for example the 1,500 m Flims, Switzerland, rock fall) and may in rare instances occur along tectonic fault zones. The occurrence of monomictic movement breccias in environments lacking tectonic fault zones and gradients sufficient for mass rock falls are strong clues to impact cratering events (Reiff 1978).

In the Azuara structure, monomictic movement breccias are very abundant. Although also found in Palaeozoic silicate rocks, they are concentrated in Triassic, Jurassic and Cretaceous limestones. An example of a typically brecciated Muschelkalk limestone is shown in Pl.1, Fig. 6. More outcrop locations of monomictic movement breccias are plotted in Fig. 5.

Impressive breccia exposures can be visited a few kilometres outside the northern ring near Belchite (UTM coordinates 6 87 000, 45 83 000; UTM coordinates 6 83 000, 45 83 000). Occasionally, large isolated blocks of Jurassic limestones emerge from the post-impact Upper Tertiary Ebro basin sediments. Quarrying in these blocks has enabled insight into the enormous impact deformations experienced by very large rock volumes. The limestones are drastically destroyed through and through to form a more or less continuous breccia displaying abundant grit brecciation and mortar texture. The uninterrupted brecciation over a distance of at least 300 m and the absence of topographic relief show that these monomictic movement breccias formed in the impact cratering process.

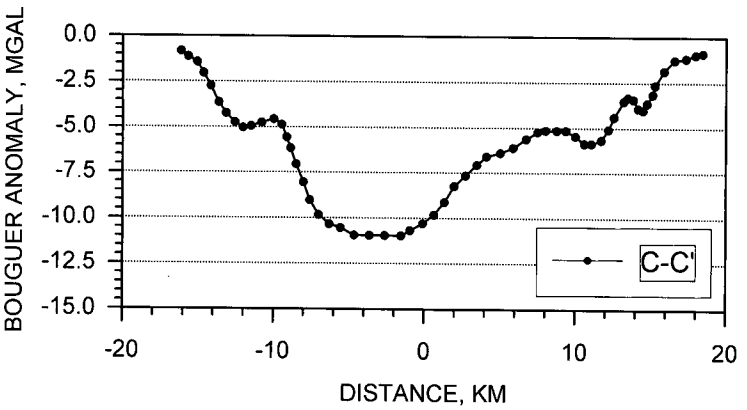

Fig. 6. Gravity profile (Bouguer residual anomalies) across the Azuara structure. Location for the profile in Fig. 5.

Fig. 6. Perfil gravitatorio (anomalies residuals de Bouguer) a través de la estructura de Azuara. La situación del perfil puede verse en la Fig. 5.

Dislocated (allochthonous) megablocks

Dislocated megablocks are characteristic of impact structures and are understood to be related to the different stages of impact cratering (excavation, ejection and modification of the transient crater; see Melosh [1989]). Thorough mapping within the Azuara structure (Bärle, 1988; Fiebag, 1988; Gwosdek, 1988; König, 1988; Linneweber, 1988; Waasmaier, 1988; Hunoltstein-Bunjevac, 1989; Müller, 1989; Katschorek, 1990; Mayer, 1991) has revealed a large number of dislocated megablocks. Gravity gliding can in most cases be excluded as an explanation, and the rootless layering of many megablocks has been shown by geophysical measurements (Bärle, 1988, König, 1988). A location map for allochthonous megablocks is given in Fig. 5. UTM coordinates of typical locations are: 6 67 350, 45 47 790, 6 70 140, 45 47 790; 6 70 390, 45 47 520; 6 77 660, 45 45 700; 6 88 850, 45 60 000, 6 69 760, 45 45 470.

Structural features

Structural features in the Azuara structure may have originated from both Alpidic tectonics and the impact cratering process. Investigations of the complete structural inventory, including folds, faults, jointing, tectonic (horizontal) stylolites, photolineations, satellite imagery, drainage pattern have been performed in detail and are discussed by Bärle (1988), Fiebag (1988), Gwosdek (1988), König (1988), Linneweber (1988), Waasmeier (1988), Hunoltstein-Bunjevac (1989), Müller (1989), Katschorek (1990), Mayer (1991), and Feld (pers. comm.). In most cases it is not possible to decide whether a distinct structural situation is related with tectonics, impact or even both, as both processes may lead to the same features (e.g., folds, faults,

joints). From impact cratering considerations (Grieve *et al.*, 1981; Melosh 1989; and many others), divergent and convergent mass transport is expected to dominate during the stages of excavation and modification, implying radial and tangential widening and shortening with respect to the crater centre. In agreement with this, these elements are frequently documented in the structural style of the Azuara structure (Fiebag, 1988, König, 1988, Katschorek, 1990, Ernstson and Fiebag, 1992) and may be related with impact rather than with tectonics. In a few cases, peculiar structural features occur, which are simply incompatible with tectonic processes (Gwosdek, 1988; Katschorek, 1990; Müller and Ernstson, 1990; Ernstson, 1994).

Geophysical data

From a gravity survey comprising 350 gravity stations, a Bouguer anomaly map of the Azuara structure has been plotted (Ernstson and Fiebag, 1992). For selected profiles, Bouguer residual anomalies were computed with the aid of provisional regional-field data (IGCE 1976, and data kindly supplied by A. Casas, Barcelona). In Fig. 6, a north to south running profile (see Fig. 5) is shown to display an overall negative anomaly of about 10 mgal amplitude. A negative gravity anomaly conforms to most other impact structures for which gravity surveys exist. Relatively positive local anomalies superimposing the main anomaly may be related with an inner ring buried beneath the young post-impact sediments of the Ebro basin (Ernstson and Fiebag, 1992). Simple model calculations and a gravity-derived mass deficiency are compatible with results for other large impact structures (Pohl *et al.*, 1978; Ernstson and Fiebag, 1992).

At each gravity station, the total intensity of the Earth's magnetic field was measured. The field contours show the central area of the Azuara structure to be practically void of anomalies. Surprisingly, short-wavelength anomalies in the periphery have considerable amplitudes exceeding 100 nT (Ernstson and Fiebag, 1992). Susceptibility measurements of a wide variety of rocks (Palaeozoic, Mesozoic and Cenozoic sediments, igneous rocks) from the Azuara structure and its environs (compilation in Hammann and Ernstson, 1987) show that highest values (k_{max} = 0.0016 S.I.) are attained in samples from the basal (suevite) breccia. Although systematic rock-magnetic studies are outstanding, a strong remnant magnetization of some basal breccia samples is observed, which is possibly a thermal remnant magnetization. Impact breccias showing stronger magnetization are known from many other impact structures. Shock pressure and post-shock temperatures are important factors that may lead to enhanced magnetization of impact breccias (Pohl 1994).

Shock metamorphism

The find of strong shock-metamorphic effects in polymictic dike breccias intercalated in Palaeozoic rocks near Nogueras and Santa Cruz de Nogueras (Ernstson *et al.*, 1985) established the impact origin for the Azuara structure. Here, we summarize new observations and investigations related to shock metamorphism in Azuara rocks. In order of decreasing shock intensity, we discuss melt glass, diaplectic crystals and

diaplectic glass, PDFs, and moderate shock effects like PFs in quartz, kinkbands in mica, and microtwinning in calcite. A discussion of moderate shatter coning in the Azuara structure is added. A general map for the occurrence of shock metamorphism is given in Fig. 7. UTM coordinates for definitive exposures are added below.

Melt glass

Melt glass in shocked breccias from the Azuara structure was first reported and described in detail by Fiebag (1988). In the polymictic dike breccias exposed near Nogueras and Santa Cruz de Nogueras (UTM coordinates, e.g., 6 61 240, 45 53 400), yellowish to reddish glass is observed to form clasts with vesicles, schlieren and mineral splinters (Pl. 2, Fig.1). Partly recrystallized glass occurs as aggregates in the matrix (Pl. 2, Fig. 2) or may coat mineral fragments. Because of the occurrence together with strongly shocked quartz (see below), the glass itself was probably formed by shock. This assumed, parts of the breccia must have experienced shock peak pressures exceeding 500 kbar (50 GPa) (Engelhardt *et al.*, 1969). Melt glass has been found also in breccia dikes exposed in the Mesozoic rim zone (Mayer, 1990) and in the basal breccia (Mayer, 1990).

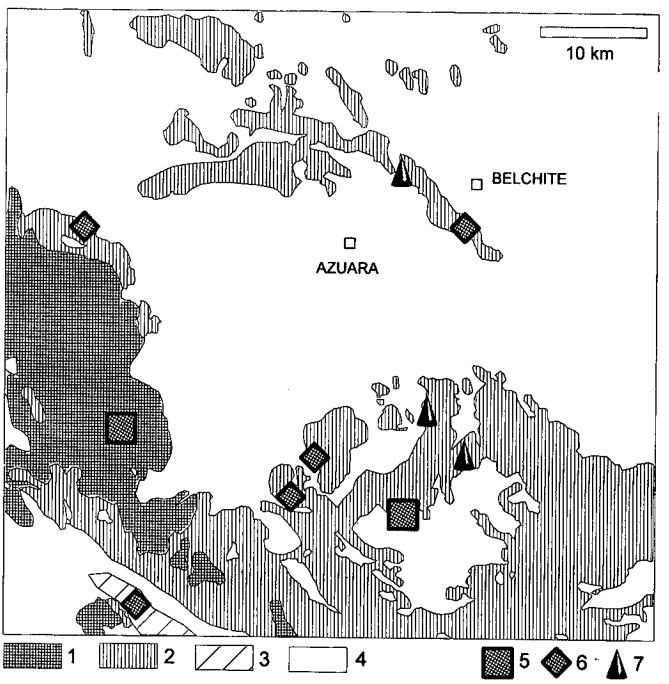

Fig. 7. Location map for strongly shocked rocks (5), moderately shocked rocks (6), and shatter cones (7). Geology same as in Fig. 4.

Fig. 7. Mapa de situación de las rocas intensamente afectadas por choque (5), rocas moderadamente chocadas (6), y conos astillados (7). La geología es la misma que la de la Fig. 4.

Diaplectic crystals and diaplectic glass

Partly (diaplectic crystals) and completely optical isotropic quartz (diaplectic glass) is abundant in breccias from the Azuara structure. Diaplectic glass was first reported by Ernstson (1994) to occur in the polymictic dike breccias near Nogueras and Santa Cruz de Nogueras, which also contain melt glass and PDFs (Pl. 2, Fig. 2). Diaplectic quartz crystals are abundant [also] in breccia dikes exposed in the Mesozoic rim zone and in the basal breccia (Mayer, 1990; and Pl. 2, Fig. 3). The formation of the amorphous quartz phase by shock without melting requires pressures of more than 15 GPa (150 kbar) for partial isotropization and 25 - 40 GPa (250 – 400 kbar) for complete transformation to diaplectic glass (Engelhardt *et al.*, 1969; Bunch *et al.*, 1968; Stöffler and Hornemann, 1972; and others).

Planar deformation features (PDFs)

Despite the clear PDFs documentation by photomicrographs and universal-stage measurements of crystallographic orientations in Ernstson *et al.* (1985), doubts about shock metamorphism in the Azuara structure were expressed by Langenhorst and Deutsch (1995). In their paper, however, all references to the shock metamorphism described in Ernstson *et al.* (1985) and in Ernstson and Fiebag (1992) are missing. Therefore, two additional independent analyses of PDFs in shocked quartz from Azuara samples (Pl. 2, Fig. 4) were performed in the Departamento de Petrología y Geoquímica, Universidad Complutense, Madrid, (by E. Guerrero Serrano) and at the Geological Survey of Canada (by A. Therriault).

Universal-stage measurements in the Madrid institution were performed on quartz of sandstone clasts from the polymictic dike breccia exposed near Santa Cruz de Nogueras (see above) and of quartzite clasts from the Pelarda Fm. ejecta (see 4.1). The prominent and prevailing $\omega\ \{10\bar{1}3\}$ and $\pi\ \{10\bar{1}2\}$ planes suggest shock pressures exceeding 10 GPa (= 100 kbar) (Stöffler and Langenhorst 1994). A. Therriault investigated quartz of sandstone and quartzite clasts also from the polymictic dike breccia and also from the Pelarda Fm. ejecta. She analyzed the crystallographic orientation of PDFs and other parameters such as their density, sharpness, spacing, and spreading over the grain. Up to five sets of PDFs per grain were observed. The spacing is 1 μm or less, the spreading over the grain in most cases 100%, and the PDF density high. Practically all sets are decorated. All shocked grains have reduced birefringence of 0.004 - 0.008. A frequency diagram for the PDF crystallographic orientation is shown in Fig. 8. Compared with the frequency diagram in Ernstson *et al.* (1985, Fig. 7), the general correspondence is obvious. Quartz grains displaying PDFs in the manner as described here, are generally considered (Stöffler and Langenhorst 1994, Grieve *et al.* 1996) to be strongly shocked, thus excluding any tectonic deformation.

Moderate shock effects

While according to current knowledge, diaplectic crystals, diaplectic glass and PDFs can form only by strong impact shock, there are mineral deformations which have been reported from both impact shock metamorphism and endogenetic processes.

Shock deformation of moderate intensity creates planar fractures (PFs, cleavage) in quartz, which belong to the regular shock inventory of impact structures. Cleavage is commonly unknown to occur in quartz. In rare cases, however, planar fractures may be produced tectonically in zones of extreme regional metamorphism. Very strong tectonic deformations may also cause kink banding in mica, which also is a typical low-grade shock effect.

Both PFs in quartz and strong kink banding in mica are abundant in rocks from the Azuara structure (Fig.7). They occur in polymictic allochthonous breccias, but also in autochthonous rocks. Waasmaier (1988) analysed 9 thin sections from Cretaceous Utrillas sandstones exposed west of Blesa and found that an average of 70 % of the micas show kink banding. In all thin sections, she observed PFs in quartz. Regularly, 2 - 3 sets occur, and in a few cases, up to six sets of different orientation per grain were observed (Pl. 2, Fig. 5). As the Cretaceous sediments have experienced Alpidic tectonics only and no regional metamorphism at all, a formation of the kinkbands and the PFs other than by shock can be excluded. The assumed shock pressures range between roughly 5 and 10 GPa (50 and 100 kbar) for the formation of PFs in quartz (Engelhardt *et al.*, 1969) and are more than 1 GPa (10 kbar) for the formation of kink bands in mica (Hörz, 1970).

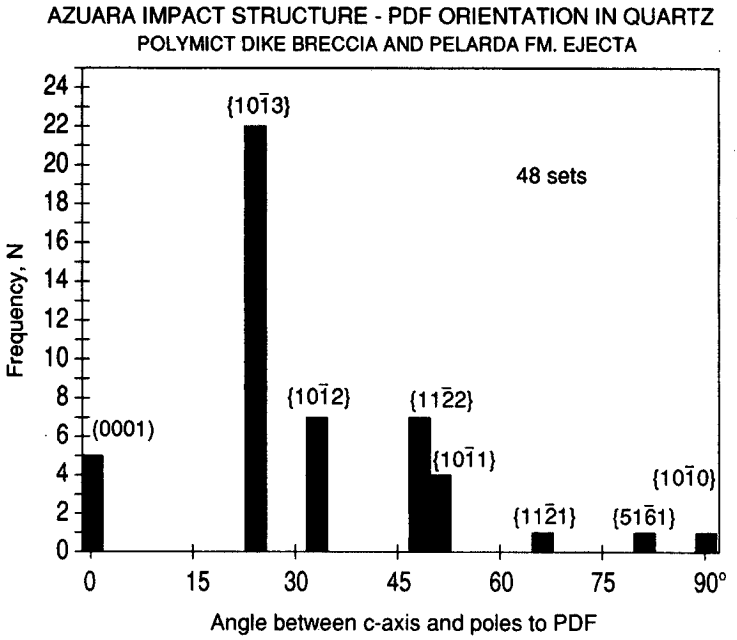

Fig. 8. Frequency diagram of crystallographic orientation of planar deformation features (PDFs) in quartz from Azuara mixed-breccia near Santa Cruz de Nogueras and from Pelarda Fm. ejecta. The diagram has been compiled from data put at our disposal by A. Therriault.

Fig. 8. Diagrama de frecuencias de la orientación cristalográfica de los rasgos de deformación planar (PDFs) presentes en cuarzos procedentes de las brechas cercanas a Santa Cruz de Nogueras y de los eyecta de la Fm. Pelarda (estructura de impacto de Azuara). El diagrama ha sido realizado a partir de los datos suministrados por A. Therriault.

Carbonate rocks are known to be less susceptible to shock-metamorphic effects. As a characteristic shock effect, microtwinning in calcite is considered (Metzler *et al.*, 1988; and references therein). Multiple sets (up to six per grain) of microtwinning in calcite from Azuara rocks are common (Pl. 2, Fig. 6) and have been reported by Fiebag (1988), Hunoltstein-Bunjevac (1989) and Mayer (1990).

Shatter cones

It is generally accepted that shatter cones form by shock waves (Roddy and Davis, 1977, Saggy *et al.*, 2002) in a pressure range between about 2 and 25 GPa (20 and 250 kbar) (Grieve, 1987). Because of thick post-impact sediments in the inner part of the Azuara structure, the finding of shatter cones is restricted to the sediments of the rim zone. In this zone, the shock wave was already weakened to the lower pressure limit of shatter-cone formation. Consequently, it is not surprising that shatter cones are rarely found and that the fracture cones often display only diffuse markings. Shatter cones in Jurassic limestones have been found at three locations (description and photographs in Mayer (1990), Katschorek (1990), Müller (1989), however in each case they were sampled from rock debris in the ring zone. The UTM coordinates of the three places are 6 84 440, 45 49 550; 6 84 700, 45 55 150; 6 83 100, 45 75 850.

THE RUBIELOS DE LA CÉRIDA IMPACT STRUCTURE

Topographic features and target rocks

The Rubielos de la Cérida structure, about 50 km south-southwest of the Azuara structure (Fig. 1), is defined by an approximately circular uplift of Mesozoic rocks (in the middle of Fig. 1), surrounded by a semi-circular to elliptical depression of Quaternary and post-impact Neogene deposits (Fig.9; simplified and modified from the geological maps 1 : 200.000; ITGE, 1991; IGME, 1986). As will be discussed later (see Impact melt rocks, Puerto Mínguez ejecta, Age of the impact event), the Neogene age of some units may be disputed. The diameter of the uplift is roughly 15 km and the west-east diameter of the depression amounts to some 40 km. The geological sketch map (Fig. 9) and a simplified section (Fig. 10) show that the existence of the central uplift is structurally controlled. In the western and northern part of the structure, its rim is made up of Mesozoic and Palaeozoic rocks belonging to the Western Iberian Chain (for the stratigraphy of the target see Fig.3). A number of hills of Mesozoic rocks emerge from the Quaternary in the western part of the depression. In the south and east, the Rubielos de la Cérida structure is less well defined. In the literature on the regional geology (ITGE, 1991; IGME, 1986; and references therein), no special account is given of the Rubielos de la Cérida structure.

Geology

In contrast with the Azuara structure, a systematic mapping of the Rubielos de la Cérida structure on 1 : 10.000 and 1 : 20.000 scales is so far lacking. A general overview is given by the geological maps on 1 : 50.000 and 1 : 200.000 scales (IGME, 1977, 1979, 1980, 1983a, 1983b, 1983c, 1986; ITGE 1991), that do not address the impact-related features. The new data presented here result from our discontinuous geologic and petrographic field work over an approximate ten year period.

Central uplift

The oldest layers exposed in the centre of the uplift are of Muschelkalk age corresponding to a stratigraphical uplift (Grieve *et al.*, 1981) of the order of 500 – 1000 m (depending on the pre-impact layering). The youngest layers are Upper Cretaceous and occur only peripherally in the west (Figs. 9, 10). From morphometrical considera-

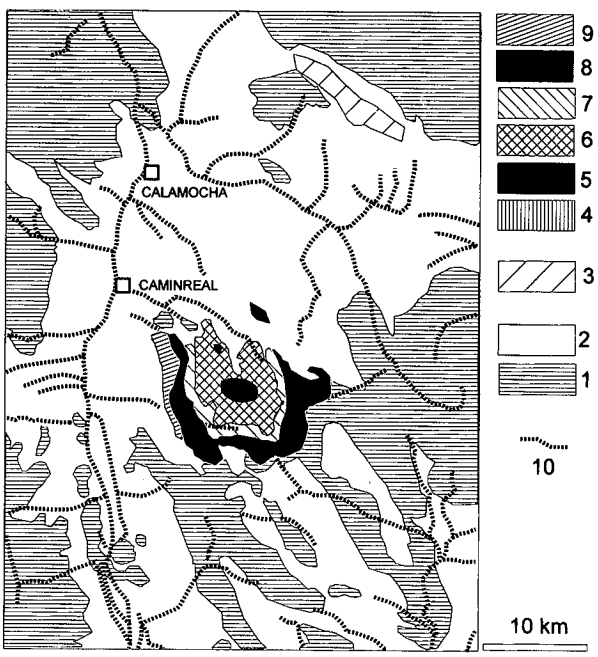

Fig. 9. Geological sketch map for the Rubielos de la Cérida impact structure, simplified and modified from ITGE (1991) and IGME (1986). 1 = Palaeozoicum, Mesozoicum and Lower Tertiary, 2 = Upper Tertiary and Quaternary, 3 = Pelarda Fm. ejecta; central uplift: 4 = Muschelkalk, 5 = Keuper, 6 = Rhaetian and Liassic, 7 = Dogger, 8 = Malmian, 9 = Cretaceous; 10 = drainage pattern.

Fig. 9. Mapa geológico de la estructura de impacto de Rubielos de la Cérida, simplificado y modificado a partir del ITGE (1991) e IGME (1986). 1 = Paleozoico, Mesozoico y Terciario inferior, 2 = Terciario superior y Cuaternario, 3 = Eyecta de la Fm Pelarda; levantamiento central: 4 = Muschelkalk, 5 = Keuper, 6 = Retiense y Liásico, 7 = Dogger, 8 = Malmiense, 9 = Cretácico; 10 = sistema de drenaje.

tions (Grieve *et al.*, 1981; Melosh, 1989), one would expect a much larger stratigraphical uplift. The divergence could possibly be related with the enormous thickness of the soft molasse top target layers (perhaps more than 2 km; see above for the data for the Azuara structure). Besides the soft argillaceous Keuper layers and a few Keuper and Cretaceous sandstones, carbonate rocks, mainly limestones, dominate.

The most significant structural feature in the central uplift is the enormous compressive signature. Strong deformation up to continuous megabrecciation is evident nearly everywhere and can best be observed in various road cuts (Pl. 3, Fig. 1). In the southern continuation of the uplift at Bueña village, deformation in the form of crisscross layering is especially impressive (Pl. 3, Fig. 2). Quarrying near the road junction CN 211 - Rubielos de la Cérida village (UTM coordinates 6 45 000, 45 20 800) reveals voluminous strong deformation (grit brecciation, mortar texture) typical of monomictic movement breccias (see the respective descriptions for the Azuara structure). About 1 km north of Rubielos de la Cérida village (UTM coordinates 640870, 4517780), quarrying has exposed a large vertical fault plane (superfault; cf. Spray, 1997) with some 300 m? of continuous mirror polish. In the contact of the plane, adjacent carbonate rocks have changed to whitish porous masses possibly as the result of decarbonization or/and melting and as such representing a variety of pseudotachylite.

On a mesoscopic scale, we observe a peculiar mechanical behaviour of limestones exposed over large areas in the uplift. On hitting them gently with a hammer two or three times, they disintegrate into innumerable small fragments and splinters as if stress was frozen within the rock.

Crater depression

Going outwards from the uplift, the remarkable deformation continues. In the Mesozoic hills emerging from the Quaternary, a number of quarries enable insight into drastic and voluminous brecciation of the limestones. In the extended quarry near Villafranca del Campo (UTM coordinates 639200; 4505200), large complexes are intensely crushed and ground to display grit brecciation and mortar texture typical of

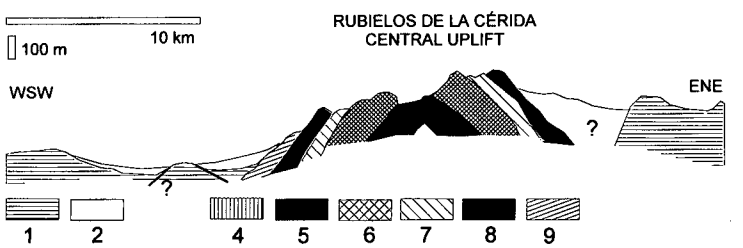

Fig. 10. Generalized geological W-E section across the Rubielos de la Cérida structure. Stratigraphical units same as in Fig. 9.

Fig. 10. Sección geológica general, de dirección E-W, a través de la estructura de Rubielos de la Cérida. Las unidades estratigráficas son las mismas que las de la Fig. 9.

monomictic movement breccias. A compressive strength of perhaps 150 - 200 MPa (= 1.5 - 2 kbar) assumed for these massive and dense Muschelkalk limestones means they must have experienced pressures clearly exceeding these values, not only locally but through and through.

Crater rims

At the rim of the depression, the rocks continue to be seen to be heavily deformed, however with varying intensity. Outcrops resulting from road construction frequently show a megabrecciation of the mostly carbonate rocks. Very often within the megabreccias, large blocks appear to have been rotated in situ, a feature also observed in the uplift.

We emphasize that such heavy and voluminous deformation is restricted to the Rubielos de la Cérida structure (and the Azuara structure) and is unknown from other regions in the Iberian chain overprinted by Alpidic tectonics.

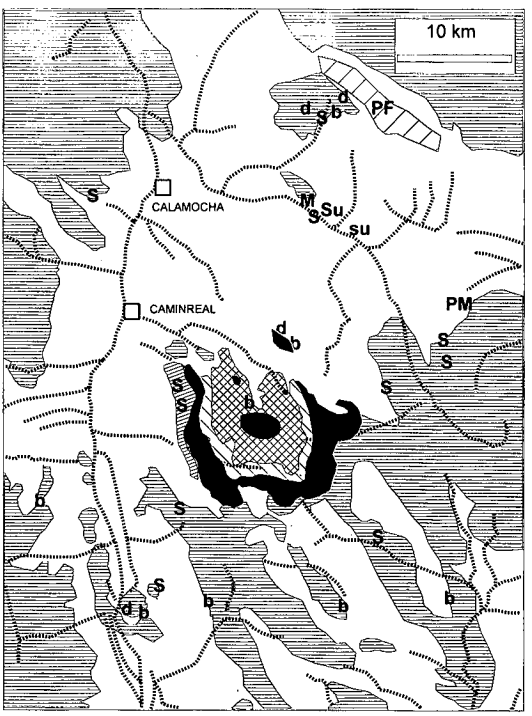

Fig. 11. Location map for impact features in the Rubielos de la Cérida structure. Geology same as in Fig. 9. PF = Pelarda Fm. ejecta, PM = Puerto Mínguez ejecta, b = basal (suevite) breccia, d = breccia dikes, M = impact melt rocks, Su = suevite, su = suevite-like impact breccia, s = shock metamorphism.

Fig. 11. Mapa de situación de los rasgos de impacto presentes en la estructura de impacto de Rubielos de la Cérida. La geologia es la misma que la de la Fig. 9. PF = Eyecta de la Fm. Pelarda, PM = Eyecta de Puerto Minguez, b = brecha basal (suevita), d = diques de brecha, M = rocas de fundido de impacto, Su = Suevita, su = suevita similar a brecha de impacto, s = metamorfismo de choque.

Breccias and breccia dikes

Apart from the widely distributed megabreccias already mentioned in the central uplift, and the voluminous monomictic movement breccias in the rim zone, breccias and breccia dikes, as described for the Azuara structure, also occur in the Rubielos de la Cérida structure. The basal (suevite) breccia is again found in immediate contact with folded Mesozoic rocks and, therefore, at the base of the post-impact (or post-Alpidic) Upper Tertiary. UTM coordinates for exposures (Fig. 11) are 6 65 650, 45 02 988; 6 59 720, 44 98 970; 6 35 870, 45 08 490.

Compared with the Azuara structure, breccia dikes seem to be less abundant, which, however, is assumed to be related to the restricted mapping activities only. Typical dikes are shown in Pl. 3, Figs. 3, 4. While the breccia dike in Pl. 3, Fig. 3 is part of an extended dike system cutting through competent Muschelkalk limestones, the dike in Pl. 3, Fig. 4 cutting through steeply dipping Jurassic limestones actually is not a *breccia* dike. The white filling of the dike is more or less homogeneously composed of highly porous, partly vesicular carbonate material without any clasts. The sharp cut and the sharp-edged fragments of the limestone, without any dissolution features exclude any karstification. Instead, the white material is suggested to be relics of crystallized carbonate melt injected into the crater wall during the excavation stage of impact cratering. The locations for breccia dikes in the Rubielos de la Cérida structure are plotted on Fig. 11. UTM coordinates for a location of breccia dikes cutting through Palaeozoic rocks near Olalla are 6 53 240, 45 37 170.

Impact melts

Impact melts were found at four locations in the Rubielos de la Cérida structure. We emphasize that these melts do not reflect the complete melt-rock spectrum in the Rubielos de la Cérida structure. As already suggested for the Azuara structure, abundant relics of former carbonate melt are proposed to also occur here in its companion crater. A carbonate melt cannot be chilled to form glass, but rapidly crystallizes to carbonate again. Therefore, the origin from a melt can only indirectly be suggested by the occurrence of skeletal, dendritic crystallites, vesicular texture and related features (see the discussion on Azuara carbonate melts by Katschorek [1990]). The melts described below are characterized by amorphous glass phases.

The host rocks

The melt-bearing rocks are exposed north of the central uplift in the valley of the Pancrudo brook roughly 10 km east of the town of Calamocha (M in Fig.11). Between the junction of the road to Cutanda/Olalla and the Barrachina village, the impact-related rocks are exposed as a megabreccia over roughly five kilometres. A further outcrop is located along the steep banks of the Pancrudo brook. On both sides of the road between the junction and Barrachina, temporary outcrops exist or have existed and may in the future be enlarged for gravel exploitation. The megabreccia is deposited

in contact with bedded sediments, which are, however, strongly folded and faulted. The term "megabreccia" refers to both the size of the components and the overall thickness, which may reach up to 50 m. Within the megabreccia, we distinguish for the present:

– a massive diamictic material which is not consolidated and has characteristics very similar to those described for the Pelarda Fm. ejecta (Ernstson and Claudin, 1990; also see 4.1) and for the ejecta deposits of the Puerto Mínguez (Claudin *et al.*, 2001; also see 4.2). As in these deposits, we observe strongly plastically deformed components which point to high confining pressures upon deformation. Occasionally, a microbreccia is intercalated, sometimes giving evidence of an injection process (Pl. 3, Fig. 5).

– This diamictic material incorporates, intermixes and interstratifies with multicoloured gypsum marls, claystones, limestones and pure gypsum (Pl. 3, Fig. 6). The multicoloured material shows a complex interlayering with the diamictic material. The deposits may overlie the diamictites, thereby tunnelling them and forming apophyses within them. Frequently, bodies of the multicoloured material are even found floating within the diamictic material. In other places, the marly material may underlie the diamictic unit. In this case, we may observe a fluidal megatexture in the diamictite obviously corresponding to a fluidal megatexture in the underlying marly unit. Very often, the impact melt rocks are embedded within this zone. Both the multicoloured composition of the megabreccia and its strange texture have much in common with the Bunte breccia ejecta of the Ries impact crater (Hüttner, 1969; Pohl *et al.*, 1977; Hörz, 1982).

– strongly brecciated limestone megablocks (Pl. 3, Fig. 7) showing a megatexture which strongly resembles grit breccias described for part of the Ries crater ejecta (Hüttner, 1969).

Silicate melt

Within the outcrop wall at the northeastern roadside (UTM coordinates 6 55 100, 45 29 900), melt rocks occur as soft, porous, fine-grained, whitish blocks of variable size in a range of decimetres up to 1 - 2 metres, intermixed in the polymictic megabreccia described above (Pl. 4, Figs. 1, 2). Two of these blocks have been investigated in detail. The rocks mainly consist of a milky white glass which forms tiny spheroids and lens-shaped bodies. Their diameters are roughly 0.5 mm (Pl. 4, Fig. 3). A second, subordinate glass phase is translucent greyish and occurs interstitial within the white glass particles (dark parts in Pl. 4, Fig. 3). The glass is estimated to make up more than 90% of the rock. This is typically shown by a distinct amorphous glass "hump", occurring in x-ray powder diffractograms (Fig. 12). Some relics of plagioclase and, to a minor extent, of quartz and mica within the glass masses are indicated by respective reflection peaks. Grains of quartz, twinned plagioclase and occasional mica are also found in thin sections of the glass matrix. In rare cases, the quartz fragments show planar deformation features (PDFs) and, more frequently, multiple sets of planar fractures (PFs). Feldspar grains show isotropization in the form of multiple sets of isotropic twinning lamellae and isotropic spots (diaplectic crystals, Pl. 2, Fig. 7), and they have

sometimes become almost completely isotropic (diaplectic glass), indicating shock peak pressures of the order of 30 GPa (300 kbar) (Engelhardt *et al.*, 1969).

Four bulk samples of the melt rocks were analyzed by RFA Philips PW1480, and separated particles of the white and the greyish glass were measured using a CAMECA SX50 electron microprobe with wavelength dispersive spectrometers at operating conditions of 15 kV accelerating voltage, 15 nA beam current and a defocussed beam size. The results are given in Table 1. Contents of Mn, Cr, Sc, Co, Ni, Mo and S are below the detection limit of the respective instrument. The poor totals of the microprobe analyses are most probably due to the presence of H_2O which entered the glass by alteration. If corrected by LOI-determination, the totals are close to 100 % as shown for the bulk analyses.

The compositions of the milky white glass spheroids and the interstitial greyish glass particles do not differ significantly. The same holds true if microprobe analyses and RFA bulk analyses are compared. Major oxides are SiO_2 between 53 and 59 wt.% and Al_2O_3 around 20 wt.%. The content of MgO in the glass particles (around 7 wt.%) is somewhat higher than in the bulk analyses (4.8 – 6.1 wt.%). Differences between the microprobe and the bulk analyses may be ascribed to secondary pore fillings or the mineral content.

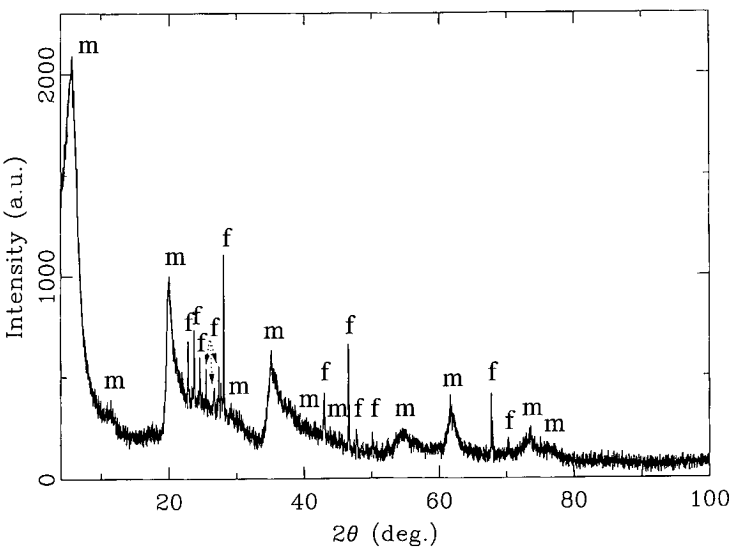

Fig. 12. X-ray powder diffractogram of the silicate melt rock shown in Pl. 4, Fig. 3. Beside the sharp diffraction peaks belonging to the feldspar phase (f), strongly broadened mica peaks (m) can be observed. The broadening reflects the low crystallinity of this phase. In the 2Q-range between 20° and 30°, a typical glass "hump" is displayed, with peaks of feldspar and mica phases superimposed.

Fig. 12. Difractograma de rayos X de la roca de fundido silicatado mostrada en la Pl. 4, Fig. 3. al lado de los picos de difracción abruptos pertenecientes a la fase feldespática (f), pueden observarse amplios picos correspondientes a las micas (m). Esta amplitud refleja la baja cristalinidad de esta fase. En el intervalo 2Q comprendido entre 20° y 30°, puede observarse un "abultamiento" típico del vidrio, con picos superimpuestos de fases de feldespato y mica.

Suevite

Silicate melt was also found in a polymictic breccia quarried out as large blocks in a temporary outcrop at the northeastern roadside in the Pancrudo valley (UTM coordinates 6 55 400, 45 29 600). Apart from the melt, the breccia is composed of matrix-supported subrounded to angular limestone, sandstone and quartzite clasts having various grain sizes. The dominantly carbonate matrix is peppered with fragmented, predominantly quartz and calcite grains, and shows flow texture with the larger clasts preferentially adjusted to the flow (Pl. 4, Fig. 4). In some cases, clasts are themselves brecciated (breccia-within-breccia). In thin sections, shock metamorphism in the form of quartz grains with multiple sets of PDFs and diaplectic quartz is observed. The melt occurs in elliptic whitish clasts with diameters between several millimetres and 2-3 cm. The soft clasts are extremely fine-grained and can easily be carved by a small spatula to get material for analysis. From x-ray powder diffraction analysis, these clasts are not pure melt, but consist of a mixture of amorphous material (typical glass hump) together with dolomite, calcite and minor amounts of quartz, muscovite and gypsum. This mixture is also reflected by the chemical bulk composition (bulk-5 analysis in Table 1). High contents of MgO and CaO and the distinct LOI values reflect dominating carbonates, mainly dolomite and subordinate calcite. The bulk-5 composition of the clasts closely matches a mixture of 50% pure dolomite, 10% pure calcite and 25% of the white glass (mean composition) in Table 1. A dominant amount of carbonates and a subordinate portion of melt is also estimated from the x-ray diffractogram. According to the current classification and nomenclature of impact rocks (IUGS Subcommission on the Systematics of Metamorphic Rocks, Study Group for Impactites), this polymictic impact breccia composed of shocked and melt clasts is termed a suevite or suevite breccia.

Suevite-like breccia

Along the road between Barrachina and Torre Los Negros, exposed limestones are strongly deformed and frequently show allochthonous material intercalated in the form of megablocks and dikes composed of multicoloured marls and shales and Palaeozoic Pelarda Fm. facies (Ernstson and Claudin, 1990; also see 4.1). At UTM 6 57 900, 45 28 300, black shales have been injected into the bedded limestones exposing a peculiar macroscopic breccia zone (Pl. 4, Fig. 5). On a smaller scale, fragmented black shales are intensively mixed with a white material to form a fine-grained breccia. In thin section, flow texture can be observed within the dark brownish to black, extremely fine-grained matrix. This matrix contains clasts of quartz and subordinate feldspar, and sometimes very fine-grained aggregates of light minerals. From x-ray powder diffraction analysis, the rock consists of quartz, kaolinite and illite, carbonate and an amorphous phase, the latter defined and documented by a typical "glass hump" (Fig. 13). Backscattered electron images of electron microprobe investigations show an extremely fine-grained mixture of medium greyish and darker greyish components on a scale of few microns. The analysis of the medium greyish parts reproducibly yields illite mixed with other clay minerals and a composition of about 53 wt.% SiO_2, 25% Al_2O_3,

5% FeO, 3% K_2O and, 2.5% each, CaO and MgO. The darker greyish parts are rich in SiO_2 and contain variable, but subordinate Al_2O_3 content. Most probably, this fine-grained mixture reflects strongly alterated relics of the amorphous (glass) phase which in an uncorroded state could not be detected by microprobe analysis. By corrosion, a glass may be transformed to clay minerals passing through an intermediate gel stage with typically enhanced Si-contents (Rösch *et al.*, 1997). No clear shock-metamorphic features have so far been identified in mineral clasts of this glass-bearing breccia. Therefore, we chose the term suevite-like breccia for this peculiar rock.

Carbonate-phosphate melt

A very special kind of former melt was found within the megabreccia of the north-eastern roadside outcrops at UTM coordinates 6 51 800, 45 31 400. The whitish melt rocks (Pl. 4, Fig. 6) are composed of irregular spheroids up to 4 mm in size, which are embedded within an extremely fine-grained matrix. Under the microscope, the spheroids

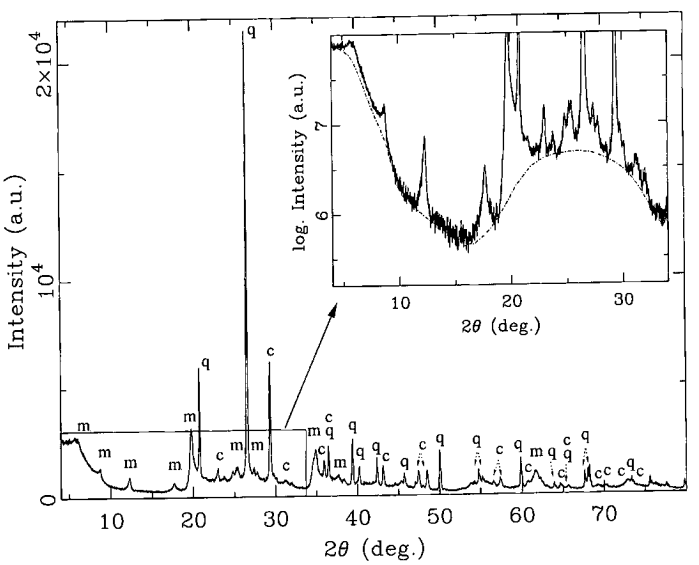

Fig. 13. X-ray powder diffractogram of the suevite-like breccia. Next to the sharp diffraction peaks of low quartz (q) and calcite (c), more or less broadened peaks of mica phases (kaolinite, illite, montmorillonite) are observed. In comparison to the silicate melt rock, a less pronounced glass "hump" is displayed due to the superimposed strong and sharp quartz and calcite peaks. The enlarged part of the diffractogram with a logarithmic scale for the intensity clearly reveals the "hump".

Fig. 13. Difractograma de rayos X correspondiente a la brecha tipo suevita. Próximos a los abruptos picos de difracción del cuarzo (q) y de la calcita (c), pueden observarse picos más o menos amplios de fases de micas (kaolinita, illita, montmorillonita). En comparación con la roca de fundido de impacto, puede observarse un "abultamiento" correspondiente a vidrio menos pronunciado debido a la fuerte y abrupta superimposición de picos de cuarzo y calcita. La parte aumentada del difractograma con una escala logarítmica para la intensidad, revela de manera clara el abultamiento.

turn out to be globular to amoeba-like calcite particles. They are coarse-grained in their centres and display decreasing grain size towards the rims. Regularly, a perpendicular grain orientation towards the rims is observed. The contact with the matrix is extremely fine-grained (Pl. 4, Fig. 7). The isotropic glass matrix in part is intensively pervaded by tiny, elongated, sometimes flaser-like microcrystals, often orientated tangentially to the rim of the calcite particles (Pl. 4, Fig. 7). The whole rock composition yields 52.7 wt.% CaO, 8.3 wt.% P_2O_5 and 1.5 wt.% BaO (RFA, bulk in Table 2). From microprobe investigations, the carbonate of the particles is pure calcite. The glassy matrix mainly consists of CaO and P_2O_5 (Table 2), with minor contents of F (1.0-2.5 wt.%), S (1.1-2.1 wt.%, if calculated as SO_3), Cl (0.5-0.8 wt.%) and NaO (0.3-0.6 wt.%). The poor totals of the analyses point to high amounts of light components within the Ca-P-glass, presumably H_2O which may have entered the glass during corrosion. The existence of considerable amounts of C or CO_2, however, must also be taken into account. Locally, a strong enrichment of Ba and S at the expense of the CaO and P_2O_5 –content is observed, which is lowered to the range of trace elements or below the detection limit, whereas Al_2O_3 is present in minor concentrations of about 1 wt.%. In part, the Ca-P-glass is recrystallized to form apatite, as verified by x-ray powder diffraction

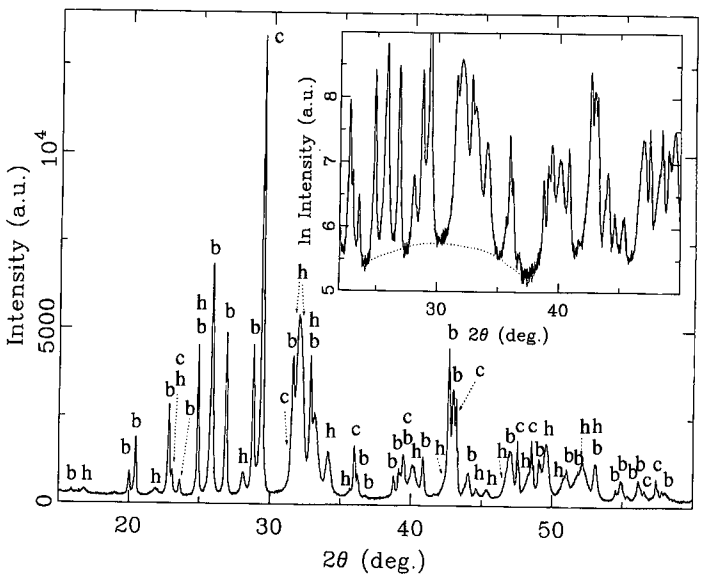

Fig. 14. X-ray powder diffractogram of the carbonate-phosphate melt. Peaks of calcite (c) and baryte (b) and distinctly broadened peaks of hydroxylapatite (h) are superimposed on a glass "hump". The "hump" shows in the enlarged part of the diffractogram with a logarithmic scale for the intensity, but is less distinct due to a subordinate content of phosphate glass in the melt.

Fig. 14. Difractograma de rayos X correspondiente al fundido de carbonato-fosfato. Pueden apreciarse picos de calcita (c), barita (b) y característicos picos amplios de hidroxiapatito (h) que se superponen sobre un "abultamiento" correspondiente a vidrio. El "abultamiento" puede observarse en la parte aumentada del difractograma con escala logarítmica para la intensidad, pero es menos ostensible debido al contenido subordinado de vidrio fosfatado presente en el fundido.

analysis. The diffraction peaks of this apatite, however, are broadened compared to those of a well crystallized one (not shown here), indicating its very low crystallinity (Fig. 14). The existence of baryte has also been proved by x-ray diffraction analysis. This baryte may occur as a very fine-grained phase within the Ba- and S-enriched locations in the Ca-P-matrix, detected by microprobe analysis.

Amorphous carbon

In the Barrachina megabreccia described above, blocks of a fine-grained microbreccia are locally intercalated. The microbreccia consists of loosely cemented carbonate and, subordinate, quartz particles. Small black clasts measuring between 0.5 and 2 mm are widespread and striking. To separate these particles from the sediment, the carbonate was dissolved in HCl and then the particles were removed from the remaining mineral fraction by hand-picking. Two kinds of black components can be distinguished. The first kind is ordinary charcoal which under the microscope shows the typical charcoal structure. Because of the weakness, the charcoal can easily be destroyed with a preparation tool, and actually, it is not of further interest for the present paper. The second kind of black particles is very hard, occurs in very irregular forms and has a surface gleaming like glass (Pl. 4, Fig. 8). Qualitative microprobe element scans show the particles to be composed of carbon and oxygen as the only major components. Additional elements are Ca in varying concentrations up to 2.7 wt.% and S varying between 0.2 and 0.8 wt.%. X-ray powder diffraction analysis of the particles resulted in diffractograms without any reflections, but showing a typical amorphous glass "hump".

Origin of the melt rocks

Silicate melt

The blocks of silicate glass are assumed to originate from melted shales. This is corroborated by the chemical composition of these melt rocks. The analyses shown in Table 1 compare quite well to a composition of shales, especially with respect to the high Al-contents and the low contents of Ca, Fe and the alkaline elements. The discrimination $\log(SiO_2/Al_2O_3)$ vs. $\log(Fe_2O_3/K_2O)$ (Herron, 1988), not shown here, also suggests that the origin of the silicate melt rocks is shale, mainly based on the low SiO_2/Al_2O_3-ratio which is typical for pelitic rocks (Wimmenauer, 1984). Using the pure SiO_2-Al_2O_3 system (compilation in Levin *et al.* [1964]), a maximum melting temperature of 1750°C can be deduced for the silicate glass rocks, which in any case is lowered due to the content of alkaline and earth alkaline elements. Very similar shock-melted shales are reported for the Haughton impact crater on Devon Island in Canada to form a highly porous network of non-transparent silicate glass with some very fine-grained particles of quartz, sheet silicates and calcite (Metzler *et al.*, 1988). Using data of Kieffer *et al.* (1976) and Stöffler (1984), a minimum shock pressure of 30 GPa (300 kbar) is required for the onset of melting in sandstones and shales, as is the case with the Haughton impact melts (Metzler *et al.*, 1988).

The Rubielos de la Cérida silicate glass rocks are clearly not of volcanic origin, due to the occurrence of strongly shocked clasts in the melt. If these melt rocks were to represent a deformed ash layer, the rocks should contain pyroclastic fragments and, with respect to an "intermediate" SiO_2-concentration, mafic relic minerals or andesitic rock fragments. Such is clearly not the case. Moreover, the chemical composition should be similar to that of andesites or basaltic andesites. Those rocks, however, generally have distinctly lower contents of Al_2O_3 and much higher contents of FeO, CaO and (Na_2O+K_2O) than the investigated silicate melt rocks (a comparison was carried out with all analyses of volcanic rocks given in Wilson [1989]). Furthermore, the melting temperature estimated for the investigated rocks does not really match the temperatures in an andesite volcanic system. Apart from impact events, the only other geologic possibility to produce melt rocks (pseudotachylites) is by frictional heating during extreme dynamic metamorphism in a thrust zone. Such a process is assumed to occur also in large impact events during the excavation and modification stages of impact cratering. The Barrachina silicate melt cannot be assumed to have formed by frictional melting of the target rocks, as the coexistence of glass and highly shocked minerals clearly speaks in favour of a shock-produced melt.

Pelitic rocks, i.e. claystones and shales, as the deduced origin of the silicate melt, are abundant in the stratigraphic sequence of the target. Only a few kilometres to the north of the Barrachina outcrops near Olalla, they contribute, for example to the Cambrian Valdemiedes and Huérmeda Fms. (ITGE 1991; Monninger 1973). They also occur in the Buntsandstein Fm., in the Upper Malmian Purbeck Facies and in the Eocene/Oligocene actually exposed in the Rubielos de la Cérida structure.

Suevite and suevite-like breccia

The melt clasts of the suevite are composed of a mixture of dolomite, calcite and glass, which is more or less similar to the silicate glass of the larger melt bodies. Carbonate, which has crystallized as calcite and dolomite, may derive from a carbonate melt. A fine-grained carbonate-rich suevite breccia with formerly melted carbonate material has been reported for the Chicxulub impact structure (Heuschkel *et al.*, 1998; Jones *et al.*, 2000) and may serve for comparison. From its macroscopic appearance, the suevite-like breccia is quite different from the suevite. Like the suevite, however, it mainly consists of a very fine-grained mixture of carbonate and silicate glass, the latter in part strongly corroded. Both breccias are composed of clasts which, apart from the melt, represent a mixture of pre-impact Palaeozoic, Mesozoic and ?Cenozoic lithostratigraphical units.

Carbonate-phosphate melt

The carbonate-phosphate rocks from Barrachina in the Rubielos de la Cérida structure do not look like typical melt rocks, and at first glance, the only hints of a former melt are the glassy relics within the phosphate matrix. The only comparable rock described up to now has been reported for the original Ries suevite, which is the melt-

bearing impact breccia of the Nördlinger Ries crater (Engelhardt *et al.*, 1969). Within this suevite, irregular, amoeba-like carbonate particles are embedded within a matrix of silicate glass. The carbonate particles show chilled margins in contact with the silicate matrix, and along this rim, calcite crystals grew elongated perpendicular to the contact. This texture was interpreted as the result of a quench crystallization (Graup, 1999), and the author was able to show that these parts of the suevite were formed by the immiscibility of impact-produced carbonate and silicate melts.

In general, the carbonate-phosphate melt rocks from Barrachina resemble the suevite from the Nördlinger Ries crater. Both rocks show these amoeba-like carbonate particles which result from quench crystallization, with chilled margins and calcite orientated perpendicular to the margin. Additionally, in both rocks, carbonate globules and carbonate particles with curvilinear rims towards the matrix occur. Like respective parts of the Ries suevite, the melt rocks from Barrachina are assumed to result from an immiscibility of two kinds of impact-induced melts, different from the Ries suevite, however, of a carbonate and a phosphate melt. A thermal decomposition of carbonates, which commences at a shock pressure of about 45 GPa (450 kbar), is also reported for the sedimentary target rocks of the Haughton impact (Metzler *et al.*, 1988; Kieffer and Simonds, 1980). At Haughton, carbonate globules and irregular blebs within silicate glass, similar to those from the Ries impact, are described and again interpreted as a result of carbonate-silicate liquid immiscibility (Osinsky and Spray, 2001a, b).

The carbonate of the carbonate-phosphate melt may be assumed to be derived from the Mesozoic, especially the Jurassic and Upper Cretaceous limestones, which are very abundant in the stratigraphic sequence of the central uplift of the Rubielos de la Cérida structure (ITGE, 1991). Limestones also occur in the Eocene (ITGE, 1991) and largely contribute to the conglomerates of the Lower Tertiary which made up a large part of the pre-impact target area (Ernstson and Fiebag, 1992). The phosphate of the carbonate-phosphate melt may be derived also from the Jurassic rocks in the target. There are two "boundary oolithes" (Geyer *et al.*, 1974) which mark the Lower/Middle and Middle/Upper Jurassic boundaries in the whole Iberian Cordillera. From these boundaries, phosphoritic components in the fossiliferous oolites are described (Geyer *et al.*, 1974). Phosphate may also originate from coprolites in the sedimentary sequence of the target. A prominent Oligocene coprolite layer has been reported, e.g., exposed near the town of Calatayud some 80 km northwest of the Rubielos de la Cérida structure (Hammann, pers. comm.). Ba, as locally observed in the carbonate-phosphate melt, is common in the target area, occurring as barite in fissures, dikes and as irregular masses in Palaeozoic rocks (ITGE, 1991).

Amorphous carbon

Carbon in elemental form, sometimes as diamonds, sometimes as C-rich shale fragments, has repeatedly been described from impact structures (Kobayashi *et al.*, 1997; Bunch *et al.*, 1997). A possible source of elemental carbon is carbonate, especially for target areas showing a thick and carbonate-rich sedimentary cover. Hypervelocity impact experiments verified the production of highly disordered graphite from dolomite or limestone targets (Bunch *et al.*, 1997). For natural impacts,

a transformation of CO to CO_2+C in the cooling atmospheric impact plume is assumed (Heymann and Dressler, 1997). Miura *et al.* (1999 a, b) propose that amorphous carbon occurring in impact structures can form from vaporized limestone target rocks in multiple impacts with reduction state. Ca-contents within the carbon are interpreted to be remains from the limestone target rocks. Thick limestone sequences in the Rubielos de la Cérida target area thus may easily have been a source for the carbon particles in the Barrachina megabreccia. This is underscored by the Ca-contents up to 2.7 wt% detected in these particles. As a further possibility and taking into account the glassy appearance and the irregular shapes of the particles, the amorphous carbon may be quenched carbon melt from extremely shocked coal of the Cretaceous Utrillas lignite deposits in the target. The melting temperature of carbon is roughly 3500°C which is exceeded at highest shock levels. The lignite layers have been of considerable economic value in Spain and are deposited roughly 20 km west of the Rubielos de la Cérida central uplift (ITGE, 1991). In the structure itself, the stratigraphically adjacent layers of Albian to Senonian age are exposed in the central uplift (ITGE, 1991), and coal-bearing Utrillas layers could have been deposited immediately at the impact point.

The role of remarkable contents of oxygen detected in the carbon particles is still unclear. Compounds of carbon and oxygen do not occur in solid state. We propose the possibility that the carbon may occur as fullerenes which are able to trap gases within their cages. Fullerenes have been reported in relation with the Sudbury impact structure and the Permian-Triassic boundary (Becker *et al.*, 1996, 2001). More investigations are necessary.

Shock metamorphism

Apart from the shock-metamorphic effects already described for the melt rocks and the suevite, moderate shock effects are regularly observed in samples from silicate rocks, mostly Cretaceous sandstones from the central uplift and the rim zone. They also occur in sandstones of the small Buntsandstein hill emerging from the Quaternary in the depression southwest of the central uplift, and the Permotriassic rocks exposed in the surroundings of Visiedo, southeast of the central uplift (erroneously mapped as Malmian there, see ITGE [1991], IGME [1979]). As in the Azuara sedimentary rocks, moderate shock is indicated by diaplectic quartz crystals (relatively rare), PDFs (relatively rare), PFs and kink bands in quartz, strong kink banding in mica, and microtwinning in calcite. In some thin sections, up to 100% of the micas are kinked. As discussed for the Azuara structure, this deformation in the Mesozoic rocks cannot possibly have resulted from Alpidic tectonics. The minerals cannot originate from reworked Palaeozoic rocks either, because they are not statistically distributed in the thin sections. Moreover, the heavily kinked micas would not have survived reworking. As additional shock effects, we observe in the Rubielos de la Cérida rocks heavily disintegrated feldspar with strong mechanical twinning and multiple sets of planar deformation features (PDF; Pl. 2, Fig. 8, also see Engelhardt *et al.* [1969], Bunch [1968], Robertson *et al.* [1968]). In Fig.11, the distribution of locations where shocked samples were taken is plotted, and UTM coordinates for selected places are given below: 6 43900, 45 03 200; 6 59 955, 45 07 300; 6 44 500, 45 10 600; 6 45 610, 45 17 600.

Shatter cones

Although competent rocks are widespread in the Rubielos de la Cérida structure and are especially well exposed in the central uplift, only very few shatter cones of moderate quality have been found so far. This is believed to be due to limited outcrop conditions (freshly exposed rocks are rare) and to the lack of a detailed mapping. Also, there may have been influencing factors which prevented shatter cone formation. We point to the assumed very thick unconsolidated molasse sediments of the target and a possible buffering effect. Moreover, we refer to the above-mentioned peculiar behaviour of the limestones in the central uplift, that is, breaking into small fragments and splinters upon hitting them gently with a hammer. The process that evidently froze stress within the limestones is unknown so far, but may have been incompatible with shatter coning.

AZUARA AND RUBIELOS DE LA CÉRIDA IMPACT EJECTA

Two impact ejecta deposits have so far been investigated in more detail: the Pelarda Fm. ejecta (Ernstson and Claudin, 1990) and the Puerto Mínguez impact ejecta (Claudin *et al.*, 2001). Both may be traced back to an early observation of an "enigmatic deposit" at Puerto Mínguez (Moissenet *et al.*, 1972). This at that time small outcrop of Palaeozoic quartzite components was also addressed by Carls and Monninger (1974) by comparing it with the Pelarda Formation. The reported similarities between the "enigmatic" Puerto Mínguez deposit and the Pelarda Fm. initiated a new thorough investigation which related the Pelarda Fm. sediments with the Azuara impact structure (Ernstson and Claudin, 1990). A completely new insight into the deposit at the Puerto Mínguez has been provided by road-construction work for the new stretch of the CN 211 between Caminreal and Montalbán. From field work in the enlarged outcrops it is suggested that the deposits are related with the Rubielos de la Cérida impact structure.

The Pelarda Fm. ejecta

The Pelarda Fm. covers an area of approximately 12 x 2.5 km? (Fig.9), has in many cases a thickness of more than 200 m and, between 1,100 and 1,450 m altitude, forms the top of a mountain chain which belongs to the highest ones in the region (Carls and Monninger, 1974). The Pelarda Fm. unconformably overlies the Fonfría Lower Tertiary (Palaeogene) which is composed of alternations of conglomerates and multicoloured marls and is overlain by the Olalla Tertiary materials (Adrover *et al.*, 1982). In the environments of Fonfría, the limestone cobbles of these conglomerates are heavily deformed and show intense striations, deep imprints and polish. The striations display more or less homogeneous SW - NE strike. In general, a lower, middle and upper zone of the Pelarda Fm. can be distinguished (Ernstson and Claudin, 1990). The contacts between the zones are gradual and not very distinct. In all three zones, stratification is completely lacking except for few conglomeratic intercalations in the

middle zone, which are more or less laminated but do not display tabular bodies (neither small nor large) nor do they form channeling structures. No structures can be observed indicating different periods of deposition (e.g., thin sandstone beds from instantaneous breaks, zones of reworked material). Likewise, a clear grain size distribution cannot be observed, and the texture is always matrix-supported (Pl. 5, Fig. 1).

In all three zones of the Pelarda Fm., cobbles and boulders are observed to display distinct striations (Pl. 5, Fig. 2). A statistical analysis of the strike for more than 400 striae sets reveals a clear maximum in the SW – NE direction (Ernstson and Claudin, 1990) which is the direction of line between the centres of both the Azuara and Rubielos de la Cérida structures. Sets of irregular, frequently open, fractures with complex bifurcations and rotated displacements (rotated fractures) occur in the cobbles and boulders, which indicate more strong plastic deformation (Pl. 5, Fig. 3). Because immediate disintegration would occur, any transport of such deformed clasts can be excluded, which proves in situ deformation.

In thin sections of quartzite cobbles and boulders (both Bámbola quartzite and Armorican quartzite), quartz grains regularly show strong mechanical deformation. We observe distinct fracturing, strong undulatory extinction, deformation lamellae, multiple sets of planar deformation features (PDFs; Pl. 5, Fig. 4) and cleavage (multiple sets of planar fractures, PFs). Kink bands in mica are frequent. The PDFs have been analyzed on the universal stage (Fig. 8) and show crystallographic orientations typical of impact shock.

From these data, Ernstson and Claudin (1990) conclude that the Pelarda Fm. constitutes the remnants of an ejecta deposit originally extended around the Azuara and Rubielos de la Cérida impact structures. The unusual thickness is explained by the interaction of the material more or less synchronously excavated from both structures.

The impact origin of the Pelarda Fm. is not generally accepted. Previous models and models opposed to an impact origin consider a Quaternary mud flow deposit of the "raña" type (Lendínez *et al.*, 1989; Pérez, 1989; Ferreiro *et al*, 1991; Aurell *et al.*, 1993; Aurell, 1994; Cortes and Martínez, 1999) and a Tertiary fluvial conglomerate (Carls and Monninger, 1974; J. Smit, 2000, written comm.). With regard to the observations and material so far presented, the interpretation of the Pelarda Fm. as a "raña" type deposit or a fluvial conglomerate implies basic problems. The almost completely missing stratification and the matrix-supported texture suggest transport by plastic (Binghamian) flow rather than fluvial transport (see Lowe, 1979; Colombo and Marzo, 1987). The observations also discard models of fluvial meander sedimentation (Miall, 1977, 1981; Bridge, 1975, 1978; Allen, 1963, 1964, 1965, 1970; McGowen and Garner, 1970) and models of braided stream sedimentation (Miall, 1977, 1978; Ramos and Sopeña, 1983; Tunbridge, 1981; Friend, 1978; Castelltort and Marzo, 1986). Sheet flood deposits as described by Friend (1983) do not occur either. The Pelarda Fm. deposit is located at the highest altitude of the region. Therefore, a fluvial or mud flow deposition requires exceptional Quaternary tectonics explicitly in this region, or sedimentation against gravity. Likewise, the suggested "raña" deposit would have developed at the base of a gradient but not on a topographic high. The observed deformation, macroscopic and microscopic (PDFs) cannot be explained by "normal tectonics", and an origin from syn-tectonic sedimentation clearly must be excluded. Moreover, given a Quaternary age of the Pelarda Fm. and considering its location at a topographic high, the overlying thick sediments required for the confining

pressure to produce the observed striations and plastic deformations have never been present. We explicitly also exclude faults (from Quaternary tectonics!) to have caused the deformations, because faults have never been observed in this zone. Also, the strike consistency of the striae throughout the huge volume of the deposit is incompatible with faulting. A formation of the striae by the action of glaciers can also be basically excluded. Otherwise, we had to establish very special conditions during the Quaternary in exactly this local zone. Moreover, and as already mentioned, the principal orientation of the striae points to the centers of both the Azuara and Rubielos de la Cérida impact structure. Large amounts of the clasts display plastic deformation (see Ernstson & Claudin, 1990) in such a manner that even a very short fluvial transport would not have been possible without complete disintegration of the clasts. Therefore, the field data suggest transport by non-Newtonian flow, contrasting with normal fluvial deposition. On the other hand, such plastic deformation has never been reported for debris flows and mud flows (McGowen and Groat, 1971; Rust, 1979; Sáez, 1985; Boothroyd and Nummedal, 1978; Miall, 1981; Heward, 1987; Bluck, 1987; Cabrera *et al.*, 1985; Gloppen and Steel, 1981). Moreover, it is very difficult to explain the rotated fractures in these clasts by normal tectonic deformation, when compared to synorogenic consolidated molasse deposits.

The Puerto Mínguez ejecta

The geological map (1 : 50.000 scale; sheet 492, Segura de los Baños) and its text explanation (IGME, 1977) report the deposits at the Puerto Mínguez as monogenetic conglomerates of Stampien age, composed of Mesozoic limestone components with large boulders included. Conglomerates of Santonian age are reported to unconformably overlie these deposits. Later, the deposits were included in the sheet of Daroca (map and text explanations at the 1 : 200.000 scale; ITGE [1991]) as Upper Oligocene to Upper Miocene materials and their origin attributed to fluvial processes. The Puerto Mínguez materials are described as "a succession of conglomerates consisting exclusively of sub-rounded limestone boulders (dimension up to 50 cm) and showing a grain-supported texture". In a recently published paper, the Puerto Mínguez deposits are classed with the sediments of the intra-mountain Montalbán basin (Casas *et al.*, 2000).

The new stretch of the road CN 211 between kilometric milestones 111 and 117 now gives easy access to the Puerto Mínguez outcrop whose aerial extent is at least 5 x 0.3 km squared. The up to several decameters thick deposits consist basically of polygenetic, weakly consolidated rudites. They show a mostly matrix-supported texture and are poorly sorted. They include conglomeratic patches, occasionally layered, as well as brecciated areas with sharp and sometimes erosive contacts. On the whole, the deposit can be termed a diamictite (Pl. 5, Fig. 5). Paleozoic materials are generally more common in the eastern part. Big clasts of prior depositional sequences, still intact, are found in the deposit, which as a whole presents poor sorting and is massive or weakly layered. Isolated Mesozoic limestone boulders in the Paleozoic-dominated clast zones are abundant (Pl. 5, Fig. 6), and frequently, like floating "islands" within the matrix, there are localised patches of conglomerates. Towards Cosa, and near the

Portalrubio junction, Palaeozoic materials become more and more scarce, until they disappear altogether. Here, the conglomeratic patches consist of large (up to meter-sized) sub-angular to sub-rounded Mesozoic limestone blocks and an increment in clast-supported texture. The patches are found dispersed in a sandy to clayey matrix, so textures are essentially matrix-supported. Side by side with these conglomerates, breccia zones are exposed (Pl. 6, Fig. 1) consisting mostly of polygenetic Palaeozoic boulders. They show various dimensions, they are matrix-supported and layering is completely lacking. Some of these breccia zones are composed of fragmented and isolated blocks, which have largely conserved their original layering. Frequently, the breccia zones are intercalated in the conglomeratic, poorly layered deposit. In other parts of the outcrop, the contacts between breccias and conglomerates are sometimes sharp and sometimes erosive.

One of the most intriguing observations, which can be made at the Puerto Mínguez deposits, is the generally strong deformation of the components, even though they are uncemented and embedded within a soft matrix. The most abundant type of deformation is the striation of the surfaces (Pl. 6, Fig. 2). Without exception, and irrespective of their size, all pebbles, cobbles and boulders of carbonate lithology are striated more or less all around. The striae have obviously originated from countermovements of components and matrix in an environment where the confining pressure was considerable. Frequently, the grains that made the striations can be found in small pits at the end of the striae path. With the decrease of the particle size of the matrix, the striated surfaces become more and more glossy, and finally they may show distinct mirror polish (Pl. 6, Fig. 3), probably due to the contact with clayey and silty matrix. The Palaeozoic components show striations as well, although less developed than those of the limestone components, probably because of the difference in lithology. Very often, imprints have formed like deep grooves and indentation hollows (Pl. 6, Fig. 4). The deep grooves seem to be caused by scraping out by matrix pebbles, and the indentation hollows seem to be caused by the penetration of an adjacent component under conditions of pure plastic deformation. Sometimes, the penetration marks resemble shapes made by a knife over soft butter. When several of these penetration marks come into contact, a faceted sculpture of the clast develops. A very unusual type of deformation that is very frequently observed in the Puerto Mínguez material, is a strong internal torsion of the components (Pl. 6, Fig. 5) which has already been described for the Pelarda Fm. ejecta (Ernstson and Claudin, 1990). The prominent torsion relates to macroscopically untouched hinges and rotated fractures, cutting through the whole cobble, without however breaking it to pieces. More irregular fractures with complex bifurcations and prominent displacements are also typical of deformed cobbles. The cobbles remain together despite squashing, a fact that we interpret as an expression of a strong confining pressure, which permits simultaneous brittle and plastic behaviour of the cobbles to the applied stress. Frequently, fractured components at first sight look like a loaf of *bread cut to slices* (Pl. 6, Fig. 6). However, the clasts are not broken to pieces at all. In many cases, widely open fractures are filled by splinters of the fractured component and matrix material, and so represent a kind of breccia dike within the cobbles. Such an interaction of matrix and clasts is typical of the Puerto Mínguez deposit, and very often, whole systems of dikes crosscut a cobble or boulder.

From the analysis of the lithologic characteristics, surface features and intense deformation of the components and the matrix of the Puerto Mínguez deposits, we conclude that the origin of these features is connected with simultaneous plastic and brittle deformation, acting rapidly, and under high contact pressure between the matrix and larger components. The rotated fractures are regarded as typical of dynamic, rapid deformation under high confining pressure. They are not compatible with an origin from fluvial deposition, quasi-static tectonics, debris flows, alluvial fans, the action of glaciers, or, generally, with syn-tectonic sedimentation (Casas *et al.*, 2000).

In summary, the Puerto Mínguez deposits are diamictites which have been deposited and deformed within a short time span and under high confining pressure. Such a setting is well known from meteorite impact ejecta. Identical depositional features and deformations (striae, polish, rotated fractures, bread-cut-to-slices features, all kinds of imprints, and others) have been described in detail for the Ries crater ejecta (Chao, 1976, 1977) and for the Belize ejecta of the Chicxulub impact structure (Marshall *et al.*, 1998; Ocampo *et al.*, 1997; Rampino *et al.*, 1996, 1997a, 1997b). For the origin of the Belize brittle and plastic deformations, the authors suggest high-velocity flow, violent collisions and shock effects as well as partially melting during excavation, transport and ballistic emplacement.

Related deposits

Deposits showing similar features as studied at the Puerto Mínguez have been observed at many other places (about 20; between the villages of Almonacid de la Cuba/Belchite in the north, Ventas de Muniesa in the east, Alfambra and Mesquita de Jarque in the south and southeast and Blancas and Daroca in the west), within the Tertiary intra-mountain basins of the region under discussion. Compared with the Puerto Mínguez, they are in general of smaller size and do not display all the features described above. Results of a more detailed investigation with reference to their position in the Tertiary stratigraphy will be presented in a forthcoming paper.

DISTANT IMPACT SIGNATURE

Originally, the observation of strongly deformed quartzite cobbles in Buntsandstein conglomerates drew attention to the Rubielos de la Cérida structure (Ernstson *et al.*, 1994). Well known to geologists, all pebbles of the Buntsandstein basal conglomerates surrounding the Azuara and Rubielos de la Cérida structures up to a distance of roughly 100 km, show distinct pock-marks and a conspicuous cratering on their surfaces. These features are obviously related to intense sub-parallel fracturing of the quartzite pebbles, both on a macroscopic and a microscopic scale (Ernstson *et al.*, 2001c). Commonly, the pock-marks and the miniature craters are explained by pressure dissolution from overburden and/or tectonic stress (IGME 1986, Cortés *et al.*, 2002b, Stel *et al.*, 2002), but Ernstson *et al.* (2001b, c; 2002) have shown that there is no evidence for this explanation. Sections and thin sections through the

cratered cobbles reveal pervasive internal fracturing, concave and subparallel spall fractures, and zones marked by quartz grains with planar deformation features (PDFs), but they fail to display the precipitation products of the alleged dissolved material. Comparison with results of impact experiments on artificial conglomerates suggests that the strong deformation is related to shock-wave propagation through the conglomerates. Accordingly, the features are explained to have occurred in the Azuara/Rubielos de la Cérida impact event by internal accelerations and multiple collisions of the cobbles producing the pock-mark indentations and spallation fractures (Ernstson *et al.*, 2001c). These observations, experiments and the discussion show that a distinct macroscopic impact signature may be found in autochthonous rocks, even at large distances from the impact sites.

THE AGE OF THE IMPACT EVENT

No radiometric absolute age is so far available for the Azuara and Rubielos de la Cérida impacts. The advanced corrosion of the glass from the impact melt rocks is expected to prevent any reliable dating.

A stratigraphic age may be addressed considering the youngest sediments affected by the impact, and the oldest undisturbed post-impact layers. A rough estimate is given by the stratigraphic position of the Pelarda Fm. ejecta at the boundary between the Lower Tertiary and the Upper Tertiary (Carls and Monninger, 1974; also see Fig. 3). According to this old and simple stratigraphic subdivision, the Lower Tertiary experienced the complete Alpidic tectonic movements, and the Upper Tertiary is the post-tectonic time, when the basins and valley systems formed with their sedimentary filling. Evidently, a comparable subdivision may apply to an impact event in this region.

Although the palaeontologic dating of Tertiary units in the Iberian chain has made progress, the stratigraphic dating still offers many problems. Explicitly, Perez *et al.*, 1985) state that the outcrops in the zone are limited and that the rapid changes of the facies prevent the use of lithological guide beds for correlation purposes. Accordingly, the exact stratigraphic age of the impact will remain unresolved for the present.

From the sediments (units 55 – 57, in ITGE [1991]) exposed near Fonfría and Allueva and underlying the Pelarda Fm. ejecta, a lower limit is Upper Eocene or earliest Oligocene (unit 57). An upper limit is given by palaeontologic data. Foraminifera and ostracods in post-impact, Upper Tertiary gastropod marls, about 3 km north of Moneva in the Azuara structure, point to a Lower Miocene age (Doebl, in Gross, 1974). A dating of the gastropods themselves (Geyer, in Gwosdek, 1988) provides an Upper Rupelian or Chattian (Oligocene) age with a high degree of probability. A position at the base of the Aquitanian, however, cannot be excluded. A further upper-limit dating is given by gastropods (Potaminidae) in Upper Tertiary sandy limestones near Ventas de Muniesa in the Azuara structure. These gastropods lived between the Upper Eocene and the earliest Miocene (Geyer, in Mayer, 1990), which does not correspond with the Middle Miocene age for the respective unit *"Areniscas en bancos, conglomerados no cementados y arcillas"* in IGME (1981). The Middle Miocene age is not palaeontologically proven. Similar problems with

Miocene ages are found also in the Rubielos de la Cérida structure. Unit 64 *"Arcillas rojas, arenas y conglomerados"* exposed south of Navarrete, is dated (ITGE, 1991) to be late Lower Miocene or Middle Miocene. Within this unit however, we observe strong structural deformations with a pronounced horizontal component (large fault planes with prominent slickensides, excluding atectonic collapse structures by karstification). This implies either remarkable tectonics in the post-tectonic Upper Tertiary, a wrong stratigraphic classification, or an origin from the impact cratering process, which, on the other hand, is questioned by Cortes *et al.* (2002), Aurell *et al.* (1993), Aurell (1994), and others.

Disregarding these incompatibilities, we conclude from the lower and upper time limits given above, that the impact event very probably occurred in the Upper Eocene or Oligocene.

CONCLUSIONS

The proximity of the Rubielos de la Cérida structure to the Azuara structure, the conspicuous location of the large ejecta complex (Pelarda Fm.), exactly in between them, the stratigraphy of the involved sedimentary units, the uniform stratigraphic age of the post-impact sediments and, especially, the widespread polymictic impact breccia at their base, suggest a Mid-Tertiary paired impact in the Upper Eocene or Oligocene, corresponding to the hitherto established age of the Azuara structure. On acceptance of this impact scenario, some basic consequences are inevitable. This is because an impact of this dimension cannot be regarded as a geologically isolated event at an isolated place (see also Ernstson [1994]). An impact of this dimension has a strong signature, which shows up with the development of small- and large-scale structural features not necessarily different from orogenic tectonics. Such a large impact also means a sudden decisive and significant break in the erosion and sedimentation history of the region under discussion. It implies the production of thick and extensive ejecta deposits (as we have seen in the above discussion), the blocking and changing of the drainage system and subsequent, long-lasting erosion and reworking processes in an area of the order of several thousands square kilometres.

Thus, the existence of a very large doublet impact structure in the region of the intra-mountain basins of the Iberian Chain is a remarkable setting in the Lower to Mid-Tertiary regional geology. As the projectiles impacted a target, which was already folded in the Alpidic orogeny and which included Tertiary basins filled with thick molasse sediments, a distinction between "normal" and "impact" geology may be problematic. This involves both the distinction between Alpidic tectonics and impact structural features on the one hand and the distinction between normal basin sediments and impact-affected sediments, on the other hand. While mountain building and impacts may lead to very similar structural features, there are observable structures and characteristics which enable deposits to be clearly established as impact-related and not to be confused with fluvial, alluvial-fan or debris-flow sedimentation. These observations can exemplarily be made with the Pelarda Fm. and the Puerto Mínguez deposits and include the peculiar layering and significant high-pressure/short-term deformations typical of impact ejecta.

The impacts, their structural features and the impact-related deposits within and outside the craters, have so far not been considered in the many models of intra-mountain syn-tectonic sedimentation, developed in the past for the region under discussion (Casas *et al.*, 2000; Pardo *et al.*, 1984; Pérez, 1989; Pérez *et al.*, 1985, 1990, 1991). We therefore conclude that these models give a rather limited picture of the Tertiary regional geology in that area, and we suggest that these specific models need revision.

ACKNOWLEDGEMENTS

The authors K.E. and F.C. want to give very heartfelt thanks for the help of a person and his team which is rather far from the world of geology. We have had long and sometimes hard field campaigns, where a good meal, a comfortable bed, and a friendly atmosphere, well beyond normal commercial standards, are paramount. So this work owes much to the Hostal Legido (at Daroca) staff. *Gracias,* Pepe and Ramón, Miguel Ángel, Alejandro, María, Josefa, and the rest of this nice group. Thanks to P. Späthe for the preparation of the thin sections and to K.-P. Kelber for several photographs shown in this paper, but also to T. Ernstson who made some important discoveries in the field. H. Müller-Sigmund, Institute of Mineralogy, Petrology und Geochemistry, University of Freiburg, carried out the qualitative microprobe element scans on the carbon particles. E. Guerrero and A. Therriault supplied abundant data from PDF analyses of Azuara samples. Reading of the manuscript by F. Guardia resulted in considerable improvements. Thank you very much for this.

REFERENCES

Adrover, R., Feist, M., Hugueney, M., Mein, P. and Moissenet, E. 1982. L'âge et la mise en relief de la formation detritique culminante de la Sierra Pelarda (Prov. Teruel, Espagne). *C. R. Acad. Sc. Paris*, **295**: 231-236.

Allen, J.R.L. 1963. The classification of cross-stratified units with notes on their origin. *Sedimentology*, **2**: 93-114.

Allen, J.R.L. 1964. Studies in fluviatile sedimentation: Six cyclothems from the Lower Old Red Sandstone. Anglo-Welsh Basin. *Sedimentology*, **3**: 163-198.

Allen, J.R.L. 1965. Fining upward cycles in alluvial successions. *Geol. J.*, **4**: 229-246.

Allen, J.R.L. 1970. *Physical processes of sedimentation.* Allen and Unwin, 248 pp.

Aurell, M. 1994. Discusión sobre algunas de las evidencias presentadas a favor del impacto meteorítico de Azuara. In: *Extinctión y registro fósil* (E. Molina, ed.), Cuadernos Interdisciplinares, **5**: 59-74, Seminario Interdisciplinar de la Universidad de Zaragoza, Zaragoza.

Aurell, M., Meléndez, A., San Roman, J., Guimera, A., Roca, E., Salas, R., Alonso, A. and Mas, R. 1992. Tectónica sinsedimentaria distensiva en el límite Triásico-Jurásico en la Cordillera Ibérica. *Actas III Cong. Geol. Esp.*, **1**, 50-54.

Aurell, M., González, A., Pérez, A., Guimerá, J., Casas, A. and Salas, R. 1993. Discussion of "The Azuara impact structure (Spain): New insights from geophysical and geological investigations" by K. Ernstson and J. Fiebag. *Geologische Rundschau*, **82**: 750-755.

Bärle, F. 1988. *Geologische Untersuchungen am SW-Rand der Azuara-Struktur (NE-Spanien). Geologische Kartierung im Maßstab 1:10.000 und spezielle Untersuchungen zur Tektonik.* Diploma thesis, 94 pp, Universität Würzburg.

Becker, L., Poreda, R. J., Bada, J. L. 1996. Extraterrestrial Helium Trapped in Fullerenes in the Sudbury Impact Structure. *Science*, **272**: 249-252.

Becker, L., Poreda, R. J., Hunt, A. G., Bunch, T. E. and Rampino, M. R. 2001. Impact event at the Permian-Triassic boundary: evidence from extraterrestrial noble gases in fullerenes. *Science*, **291**: 1530 – 1533.

Bischoff, L. and Oskierski W., 1987. Fractures, pseudotachylite veins and breccia dikes in the crater floor of the Rochechouart impact structure, SW-France, an indicator of craterforming processes. In: *Research in Terrestrial Impact Structures*, (J. Pohl, ed.), 5-29, Braunschweig (F. Vieweg & Sohn).

Bischoff, L. and Oskierski, W. 1988. The surface structure of the Haughton impact crater, Devon Island, Canada. *Meteoritics*, **23**: 209-220.

Bluck, B. J. 1987. Fan lithosome geometry as function of tectonics. *Alluvial fans and their tectonic controls*. Joint meeting BSRG and TGG Bristol University, October, 17, 1987. Abstracts, 4 pp.

Boothroyd, J.C. and Nummedal, D. 1978. Proglacial braided outwash – a model for humid alluvial fan deposits. In: Miall, A.D. ed, *Fluvial Sedimentology.* Mem. Can. Soc. of Petrol. Geol., **5**: 641-668.

Bridge, J. S. 1975. Computer simulation of sedimentation in meandering streams. *Sedimentology*, **22**: 3-44.

Bridge, J. S. 1978. Paleohydraulic interpretation using mathematical models of contemporary flow and sedimentation in meandering channels. In: Miall, A.D. ed, *Fluvial Sedimentology.* Mem. Can. Soc. Petrol. Geol., **5**: 723-742.

Bunch, T. E. 1968. Some characteristics of selected minerals from craters. In: French, B. M. and Short, N. M. (eds.), *Shock Metamorphism of Natural Materials.* Mono Book Corp., Baltimore, 413-432.

Bunch, T. E., Becker, L., Schultz, P. H. and Wolbach, W. S. 1997. New potential sources for Black Onaping carbon. *Large Meteorite Impacts and Planetary Evolution*, 30. 8. – 5. 9. 1997, Sudbury, abstracts.

Cabrera, LL., Colombo, F. and Robles, S. 1985. Sedimentation and Tectonics interrelationships in the Paleogene marginal alluvial systems of the SE. Ebro Basin. Transition from alluvial to shallow lacustrine environments. In: J. Rosell and M. Milá (eds.): *6th European IAS Meeting. Lleida. Spain. Excursion Guidebook.* Exc, 10: 394-492.

Carls, P. 1965. *Jung-silurische und unterdevonische Schichten der östlichen Iberischen Ketten (NE-Spanien).* - Doctoral Thesis, Univ. Würzburg. 155 pp.

Carls, P. 1983. La zona asturoccidental-leonesa en Aragon y el macizo del Ebro como prolongación del macizo cantabrico. In: *Libro Jubilar J. M. Ríos, (Comisión Nacional de Geologia, ed.), Contribuciones sobre temas generales*, Inst. Geol. Miner. Espana, **III,** 11—32, Madrid.

Carls, P. and Monninger, W. 1974. Ein Block-Konglomerat im Tertiär der östlichen Iberischen Ketten (Spanien). *N. Jb. Geol. Paläont. Abh.*, **145**: 1-16.

Casas, A.M., Casas, A., Pérez, A., Tena, S., Barrier, L., Gapais, D. and Nalpas, T., 2000. Syn-tectonic sedimentation and thrust-and-fold kinematics at the intramountain Montalbán Basin (northern Iberian Chain, Spain). *Geodinamica Acta,* **1**: 1-17.

Castelltort, F.X. and Marzo, M. 1986. Un modelo deposicional de abanicos aluviales arenosos originados por corrientes efímeras: el Muschelkalk medio de los Catalanides. *XI Congr. Español de Sedimentología.* Resúmenes y comunicaciones, 47.

Chao, E. C. T. 1976. Mineral produced high pressure striae and clay polish: Key evidence for nonballistic transport of ejecta from Ries crater. *Science*, **194**: 615-618.

Chao, E.C.T. 1977. The Ries crater of southern Germany. A model for large basins on planetary surfaces. *Geol. Jb.*, **A43**: 81 pp.

Claudin, F., Ernstson, K., Rampino, M. R. and Anguita, F. 2001. Striae, polish, imprints, rotated fractures, and related features from clasts in the Puerto Minguez impact ejecta in NE Spain, in: *Impact markers in the stratigraphic record, 6th ESF-IMPACT workshop Granada, abstract book*: 15-16.

Colombo, F. and Marzo, M. 1987. Conceptos básicos de fluidodinámica y tipos principales de flujos. In: J. Martí (ed.): *Curso de postgrado de Volcanología*, tomo 2: 1-104. Opt. Geoquímica, Petrología y Prospección geológica. Fac. Geología Universitat de Barcelona.

Cortes, A.L. 1994. *Geometría y cinemática de las estructuras alpinas en el sector Cariñena-Belchite (Borde norte de la Cordillera Ibérica).* Tesis de Licenciatura, Universidad de Zaragoza, 171 pp.

Cortés, A.L. and Martínez, M.B. 1999. Controversia científica para el aula: ¿tiene la cubeta de Azuara un origen extraterrestre? *Enseñanza de las Ciencias de la Tierra,* **7.2**: 143-157.

Cortés, A. L., Díaz-Martínez, E., Sanz-Rubio, E., Martínez-Frías, J. and Fernández, C. 2002a. Cosmic impact versus terrestrial origin of the Azuara structure (Spain): A review. *Meteoritics Planet. Sci.*, **37**: 875-894.

Cortés, A. L., Díaz-Martínez, E., González-Casado, J. M., Aurell, M. and Casas-Sainz, A. M. 2002b. Cratered cobbles in Triassic Buntsandstein conglomerates in northeastern Spain: An indicator of shock deformation in the vicinity of large impacts: Comment. *Geology*, **30**: 91.

Dressler, B. O. (1970). *Die Beanspruchung der präkambrischen Gesteine in der Krypotexplosionsstruktur von Manicouagan in der Provinz Quebec, Kanada.* Doctoral Thesis, Univ. München.

Dressler, B. O. 1984. The effects of the Sudbury event and the intrusion of the Sudbury igneous complex on the Footwall rocks of the Sudbury structure. In: *The Geology and Ore Deposits of the Sudbury Structure* (E. G. Pye, A. J. Naidrett and P. E. Giblin, eds.), Ontario Geological Survey Spec. Vol. **1**, 97-136.

Engelhardt, W. v., Stöffler, D. and Schneider, W. 1969. Petrologische Untersuchungen im Ries. *Geologica Bavarica,* **61**: 229-295.

Ernstson, K. 1994. Looking for geological catastrophes: The Azuara impact case. In: *Extinción y registro fósil* (E. Molina, ed.), Cuadernos Interdisciplinares, **5**: 31-57, Seminario Interdisciplinar de la Universidad de Zaragoza, Zaragoza.

Ernstson, K. and Claudín, F. 1990. Pelarda Formation (Eastern Iberian Chains, NE Spain): Ejecta of the Azuara impact structure. *N. Jb. Geol. Paläont. Mh.*, **1990**: 581-599.

Ernstson, K. and Fiebag, J. 1992. The Azuara impact structure: New insights from geophysical and geological investigations. *Geol. Rundschau*, **81**: 403-427.

Ernstson, K. and Fiebag, J. 1993. Reply to discussion of "The Azuara impact structure (Spain): new insights from geophysical and geological investigations" by Aurell, M., González, A., Pérez, A., Guimerà, J., Casas, A. and Salas, R. (1993). *Geol. Rundschau*, **82**: 756-759.

Ernstson, K., and Hiltl, M. 2002. Cratered cobbles in Triassic Buntsandstein conglomerates in northeastern Spain: An indicator of shock deformation in the vicinity of large impacts: Reply. *Geology*, **30**: 1051-1052.

Ernstson, K., Hammann, W., Fiebag, J. and Graup, G. 1985. Evidence of an impact origin for the Azuara structure (Spain). *Earth Planet. Sci. Let.*, **74**: 361-370.

Ernstson, K., Feld, H. and Fiebag, J. 1987. Impact hypothesis for the Azuara structure (Spain) strengthened. *Meteoritics*, **22**: 373.

Ernstson, K., Anguita, F. and Claudín, F. 1994. Shock cratering of conglomeratic quartzite pebbles and the search for and identification of an Azuara (Spain) probable companion impact structure. European Science Foundation Network: Impact cratering and evolution of Planet Earth. Third International Workshop on *Shock wave behaviour of solids in nature and experiments*, Limoges, France. Abstract book, p. 25.

Ernstson, K., Claudin, F., Schüssler, U., Anguita, F. and Ernstson, T. 2001a. Impact melt rocks, shock metamorphism, and structural features in the Rubielos de la Cérida structure, Spain: evidence for a companion to the Azuara impact structure, in: *Impact markers in the stratigraphic record, 6th ESF-IMPACT workshop Granada, abstract book*: 23-24.

Ernstson, K., Rampino, M. R. and Hiltl, M. 2001b. Shock-induced spallation in Triassic Buntsandstein conglomerates (Spain): an impact marker in the vicinity of large impacts, in: *Impact markers in the stratigraphic record, 6th ESF-IMPACT workshop Granada, abstract book*: 25-26.

Ernstson, K., Rampino, M. R., and Hiltl, M. 2001c. Cratered cobbles in Triassic Buntsandstein conglomerates in northeastern Spain: An indicator of shock deformation in the vicinity of large impacts. *Geology*, **29**: 11-14.

Ernstson, K., Rampino, M. R., and Hiltl, M. 2002. Cratered cobbles in Triassic Buntsandstein conglomerates in northeastern Spain: An indicator of shock deformation in the vicinity of large impacts: Reply. *Geology*, **30**: 92.

Fiebag, J. 1988. *Zur Geologie der Azuara-Struktur (NE-Spanien). Kartierung im Gebiet zwischen Herrera de los Navarros und Aladrén und süd-östlich von Almonacid de la Cuba sowie spezielle Untersuchungen der Breccien und Breccien-Gänge vor dem Hintergrund einer Impaktgenese der Azuara-Struktur.* Doctoral thesis, 271 pp., Fak. Geowiss., Universität Würzburg.

French, B. M. and Short, N. M. (eds.) 1968. *Shock Metamorphism of Natural Materials*. Mono Book Corp., Baltimore, 644 pp.

Friend, P.F. 1978. Distinctive features of some ancient rivers systems. In: Miall, A.D. ed, *Fluvial Sedimentology.* Mem. Can. Soc. Petrol. Geol., **5**, 531-542.

Friend, P. F., 1983, Towards the field classification of alluvial architecture or sequence. In Collinson, J. D., and Lewin, J., eds., *Modern and Ancient Fluvial Systems:* Boston, Blackwell Scientific Publ., 345-354.

Geyer, O. F., Behmel, H. and Hinkelbein, K. 1974. Beiträge zur Stratigraphie und Paläontologie des Juras von Ostspanien. VII. Die Grenzoolithe im Jura von Ostspanien. *N. Jb. Geol. Paläont. Abh.*, **145**: 17-57.

Gloppen, T. G. and Steel, R. J. 1981. The deposits, internal structure and geometry in six alluvial fan-delta bodies (Devonian-Norway) - a study in the significance of bedding sequence in conglomerates. In: F. G. Ethridge and R. M. Flores (eds): *Recent and ancient nonmarine depositional environments: Models for exploration.* Society of Economic. Paleontologist and Mineralogists Special Publication, **31**: 49-69.

Goy, A., Gomez, J.J.and Yebenes, A. 1976. El Jurásico de la Cordillera Ibérica (mitad norte): unidades litoestratigráficas. *Estud. Geol.*, **32**: 391-423.

Graup, G. 1999. Carbonate-silicate liquid immiscibility upon impact melting: Ries Crater, Germany. *Meteoritics Planet. Sci.*, **34**: 425-438.

Grieve, R. A. F. 1982. The record of impact on Earth: implications for a major Cretaceous/Tertiary impact event. In: *Geological Implications of Impacts of Large Asteroids and Comets on the Earth* (L.T. Silver and P.H. Schultz, eds.), Geol. Soc. Amer., Spec. Pap., **190**: 25-37.

Grieve, R. A. F. 1987. Terrestrial impact structures. *Ann. Rev. Earth Planet. Sci.*, **15**: 245-270.

Grieve, R. A. F. and Robertson, P. B. 1979. The terrestrial cratering record. I. The current status of observation. *Icarus*, **38**: 212-229.

Grieve, R. A. F., Robertson, P. B. and Dence, M. R. 1981. Constraints on the formation of ring impact structures, based on terrestrial data. In: *R.B. Merrill, P. H. Schultz (Eds.), Multi-ring Basins,* Lunar Planet. Sci. Proc. 12A, Pergamon Press, New York, 37-57.

Grieve, R.A.F., Langenhorst, F. and Stöffler D. 1996. Shock metamorphism of quartz in nature and experiment: II. Significance in geoscience. *Meteoritics & Planet Sci,* **31**: 6-35.

Gross, G. 1974. Untersuchungen zur Stratigraphie und Genese der tertiären Sedimentgesteine im Ebrobecken (NE-Spanien). *N. Jb. Geol. Paläont. Abh.*, **145**: 243-278.

Gwosdek, C. 1988. *Geologische Untersuchungen am SE-Rand der Azuara-Struktur (NE-Spanien). Erläuterungen zu einer Kartierung (1:10.000) in der Umgebung von Moneva mit besonderer Berücksichtigung der tektonischen Verhältnisse.* Diploma thesis, 108 pp., Universität Würzburg.

Hammann, W. and Ernstson, K. 1987. *Untersuchungen der Geologie und Geophysik im Gebiet der vermuteten Impakt-Struktur Azuara (NE-Spanien).* DFG-Tätigkeitsbericht, 26 pp.

Herron, M. M. 1988. Geochemical classification of terrigenous sands and shales from core or log data. *J. Sed. Petrol.*, **58**: 820-829.

Heuschkel, S., Lounejeva Baturina, E., Jones, A. P., Sanchez-Rubio, G., Claeys, P. and D. Stöffler, D. 1998. Carbonate melt in the suevite breccia of the Chicxulub crater. *Eos Trans. AUG*, **79** (45), Fall Meet. Suppl.: F554.

Heward, A.P. 1987. Alluvial fan sequence and megasequence models: with examples from Westphalian D Stephanian B coalfields, northern Spain. In: Miall, A.D. ed, *Fluvial Sedimentology.* Mem. Can. Soc. Pet. Geol., **5**: 669-702.

Heymann, D. and Dressler, B. O. 1997. Origin of carbonaceous matter in rocks from the Whitewater Group of the Sudbury structure. *Large Meteorite Impacts and Planetary Evolution,* 30. 8. – 5. 9. 1997, Sudbury, abstracts.

Hörz, F. 1970. Static and dynamic origin of kink bands in micas. *J. Geophys. Res.*, **75**, 965- 977.

Hörz, F. 1982. Ejecta of the Ries Crater, Germany. In: *Geological Implications of Impacts of Large Asteroids and Comets on the Earth* (L.T. Silver and P.H. Schultz, eds.), Geol. Soc. Amer., Spec. Pap., **190**: 39-55.

Hradil, K., Schüssler, U. and Ernstson, K. 2001. Silicate, phosphate and carbonate melts as indicators for an impact-related high-temperature influence on sedimentary rocks of the Rubielos de la Cérida structure, Spain, in: *Impact markers in the stratigraphic record, 6th ESF-IMPACT workshop Granada, abstract book*: 49-50.

Hüttner, R. 1969. Bunte Trümmermassen und Suevit. *Geol. Bavarica*, **61**: 142-200.

Hunoltstein-Bunjevac, D. von. 1989. *Geologische Untersuchungen am SE-Rand der Azuara-Struktur (NE-Spanien). Erläuterungen zu einer Kartierung (1:10.000) in der Umgebung von Moneva unter besonderer Berücksichtigung struktureller Merkmale.* Diploma thesis, 111 pp., Universität Würzburg.

IGCE. 1976. Mapa gravimétrico, Península Ibérica e Islas Baleares. Anomalías Bouguer Sistema, 1967.

IGME. 1977. Memoria hoja n.° 492 (Segura de los Baños) del Mapa Geológico de España. 1:50.000.

IGME. 1978. Memoria hoja n.° 517 (Argente) del Mapa Geológico de España. 1:50.000.

IGME. 1981. Memoria hoja n.° 40 (Daroca) del Mapa Geológico de España. 1:200.000.

IGME. 1983. Memoria hoja n.° 516 (Monreal del Campo) del Mapa Geológico de España. 1:50.000.

IGME. 1986. Memoria hoja n.° 47 (Teruel) del Mapa Geológico de España. 1:200.000.

ITGE. 1991. Memoria hoja n.° 40 (Daroca) del Mapa Geológico de España. 1:200.000.

Jones, A. P., Claeys, P. and Heuschkel, S. 2000. Impact melting of carbonates from the Chicxulub crater, in: Gilmour, I. and Koeberl, C. (Ed.) *Impacts and the Early Earth.* Series: Lecture Notes in Earth Sciences, Vol. **91**, Springer, Heidelberg, 445 pp.

Katschorek, T. 1990. *Geologische Untersuchungen am N-Rand der Azuara-Struktur (NE-Spanien). Erläuterungen zu einer Kartierung 1 : 20.000 des Gebietes zwischen Fuendetodos und Belchite unter besonderer Berücksichtigung struktureller Merkmale.* Diploma thesis, 198 pp., Universität Würzburg.

Kieffer, S. W. and Simonds, C. S. 1980. The role of volatiles and lithology in the impact cratering process. *Review of Geophys. and Space Physics*, **18**: 143-181.

Kieffer, S. W., Phakey, P. P.and Christie, J. M. 1976. Shock process in porous quarzite: Transmission electron microscope observations and theory. *Contrib. Mineral. Petrol.*, **59**: 41-93.

Kobayashi, H., Miura, Y. and Fukuyama, S. 1997. Large CVD diamond-like carbon formed by multi-impact reactions. *Large Meteorite Impacts and Planetary Evolution*, 30. 8. – 5. 9. 1997, Sudbury, abstracts.

König, R. 1988. *Geologische Untersuchungen am SW-Rand der Azuara-Struktur (NE-Spanien). Geologische Kartierung im Maßstab 1 : 10.000 und spezielle Untersuchungen zur Tektonik.* Diploma thesis, 142 pp., Universität Würzburg.

Lambert, P. 1981. Breccia dikes: geological constraints on the formation of complex craters. In: *R.B. Merrill, P. H. Schultz (Eds.), Multi-ring Basins,* Lunar Planet. Sci. Proc. 12A, Pergamon Press, New York, 59-78..

Langenhorst, F. and Deutsch, A. 1996. The Azuara and Rubielos structures, Spain: Twin impact craters or Alpine thrust systems? TEM investigations on deformed quartz disprove shock origin (abstract). *Lunar and Planetary Science, v. XXVII*: 725-726.

Lendínez, A., Ruiz, V. and Carls, P. 1989. Mapa y memoria explicativa de la hoja 439 (Azuara) del Mapa Geológico de España a escala 1:50000. ITGE. Madrid. 42 pp.

Levin, E. M., Robbins, C. R. and McMurdie, H. F. 1964. *Phase diagrams for ceramists.* Amer. Ceram. Soc., Columbus Ohio, 1964, 601 pp.

Linneweber, S. 1988. *Geologische Untersuchungen am SE-Rand der Azuara-Struktur (NE-Spanien). Erläuterungen zu einer Kartierung (1 : 10.000) im Gebiet zwischen Blesa und Muniesa mit besonderer Berücksichtigung der tektonischen Verhältnisse.* Diploma thesis, 103 pp., Universität Würzburg.

Lowe, D.R. 1979. Sediment gravity flows: Their classification and some problems of application to natural flows and deposits. In: L.J. Doyle and D.H. Pilkey (eds): *Soc. Econ. Paleont. Miner. Special Publication.*, **27**: 75-82.

Marshall, J.R., Bratton, C., Pope, K.O. and Ocampo, A.C. 1998. Diagnostic clast-texture criteria for recognition of impact deposits. *Lunar Planet. Sci. Conf., XXIX*, Abstract No. 1134.

Mayer, G. 1991. *Geologische Untersuchungen am SE-Rand der Azuara-Struktur (NE-Spanien). Geologische Kartierung im Maßstab 1 : 20.000 unter besonderer Berücksichtigung der tektonischen Verhältnisse und vor dem Hintergrund einer Impaktgenese der Struktur.* Diploma thesis, 216 pp., Universität Würzburg.

McGowen, J.H. and Garner, L.E. 1970. Physiographic features and stratification types of coarse grained point bars; modern an ancient examples. *Sedimentology*, **14**: 77-111.

McGowen, J.H. and Groat, C.G. 1971. Van Horn Sandstone, West Texas, an alluvial fan model for mineral exploration. *Texas Bureau of Economic Geology Report of Investigations*, **72**: 57 pp.

Melosh, H.J. 1989. *Impact cratering. A geologic process.* Oxford Univ. Press, Oxford, 245 pp.

Metzler, A., Ostertag, R., Redeker, H.-J. and Stöffler, D. 1988. Composition of crystalline basement and shock metamorphism of crystalline and sedimentary target rocks at the Haughton impact crater, Devon Island, Canada. *Meteoritics*, **23**: 197-207.

Miall, A.D. 1977. A review of the braided-river depositional environment. *Earth-Sci. Rev*, **13**: 1-62.

Miall, A.D. 1978. Lithofacies types and vertical profile models in braided river deposits: a summary. In: Miall, A.D. ed, *Fluvial Sedimentology.* Mem. Can.Soc. Petrol. Geol., **5**: 597-604.

Miall, A.D. 1981. Analysis of fluvial depositional systems. *Am. Ass. Petrol. Geol., Fall education conference*, Calgary, 75 pp.

Miura, Y., Fukuyama, S. and Gucsik, A. 1999. Compositional changes by multiple impacts. *J. Materials Processing Technol.*, **85**: 192-193.

Miura, Y., Kobayashi, H., Kedves, M. and Gucsik, A. 1999. Carbon source from lime-stone target by impact reaction at the K/T boundary. *Lunar and Planet. Sci. Conf. XXX:* 1522-1523.

Moissenet, E., Canerot, J. and Pailhé, P. 1972. Géologie et relief dans la région de Montalbán (province de Teruel). *Melanges Casa Velasques*, **8**: 1-47.

Monninger, W. 1973. *Erläuterungen zur geologischen Kartierung im Gebiet um Olalla (Prov. Teruel) (NE-Spanien),* Diploma thesis, Univ. Würzburg, 1973, 140 pp.

Müller, H. 1989. *Geologische Untersuchungen am SE-Rand der Azuara-Struktur (NE-Spanien). Geologische Kartierung im Maßstab 1 : 20.000 zwischen Ventas de Muniesa und Moneva unter besonderer Berücksichtigung struktureller Merkmale.* Diploma thesis, 167 pp., Universität Würzburg.

Müller, H. and Ernstson, K. 1990. Curved joint sets: Indication of impact-induced fracturing. In: *Proceedings Int. Conf. on Mechanics of Jointed and Faulted Rock,* April 18-20, 1990, Vienna, (H. S. Rossmanith, ed.). Balkema, Rotterdam, 257-263.

Ocampo, A.C., Pope, K.O. and Fischer, A.G. 1997. Carbonate ejecta from the Chixculub crater: Evidence for ablation and particle interactions under high temperatures and pressures. *Lunar Planet. Sci. Conf., XXVIII:* 1035 - 1036.

Osinski, G. R. and Spray, J. G. 2001a. Impact-generated carbonate melts: evidence from the Haughton structure, Canada. *Earth Planet. Sci. Let.*, **194**: 17-29.

Osinski, G. R. and Spray, J. G. 2001b. Highly shocked low densitiy sedimentary rocks from the Haughton impact structure, devon Island, Nunavut, Canada. *Lunar Planet. Sci. Conf. XXXII,* Lunar Planet. Inst. Houston, abstract 1908.

Pardo, G., Villena, J., Perez, A. and Gonzalez, A. 1984. El Paleógeno de los margenes del umbral de Montalbán: relación tectónica-sedimentación. *Publ. de Geol.*, **20**: 355-363.

Pérez, A. 1989. *Estratigrafía y sedimentología del Terciario del borde meridional de la Depresión del Ebro (sector riojano-arogonés) y cubetas de Muniesa y Montalbán.* Tesis Doctoral, Universidad de Zaragoza, 525 pp.

Pérez, A., Azanza, B., Cuenca, G., Pardo, G. and Villena, J. 1985. Nuevos datos estratigráficos y paleontológicos sobre el Terciario del borde meridional de la Depresión del Ebro (provincia de Zaragoza). *Est. Geol.*, **41**: 405-411.

Pérez, A., Pardo, G. and Villena J. 1990. El Terciario de la cubeta de Muniesa (provincia de Teruel). *Geogaceta*, **8**: 100-101.

Pérez, A., Muñoz, A., González, A., Pardo, G. and Villena, J. 1991. Interpretación tectonosedimentaria de la Depresión Terciaria de Azuara. Margen Ibérico de la cuenca del Ebro. Provincia de Zaragoza. *Actas I Cong. Grupo Esp. Terc.*, 229-232.

Pohl, J. 1994. The effect of shock on magnetic properties of rocks and minerals. European Science Foundation Network: Impact cratering and evolution of Planet Earth. Third International Workshop on *Shock wave behaviour of solids in nature and experiments*, Limoges, France. Abstract book, p. 51.

Pohl, J., Stöffler, D., Gall, H. and Ernstson, K. 1977. The Ries impact crater. In: *Impact and Explosion Cratering* (D.J. Roddy, R.O. Pepin, R.B. Merrill, eds.), Pergamon Press, New York, 343 - 404.

Pohl. J., Ernstson, K. and Lambert, P. 1978. Gravity measurements in the Rochechouart impact structure (France). *Meteoritics*, **13**: 601-604.

Ramos, A. and Sopeña, A. 1982. Gravel bars in low sinuosity streams (Permian and Triassic, central Spain). In: *Modern and Ancient Fluvial Systems* (Miall, A.D Collinson, J. D. and Lewin, J.). Spec. Publ. Int. Ass. Sediment., **6**: 301-312.

Rampino, M.R., Ernstson, K., Fischer, A.G., King, D.T., Ocampo, A., and Pope, K.O. 1996. Characteristics of clasts in K/T debris-flow diamictites in Belize compared with other known proximal ejecta deposits. *Abstracts with Prog., Geol. Soc. Am.*, **28**: A-182.

Rampino, M. R., Ernstson, K., Anguita, F., and Claudín, F. 1997a. Striations, polish, and related features of clasts from impact-ejecta deposits and the "tillite problem". *Conference on Large Meteorite Impacts and Planetary Evolution*, Sudbury, Ontario, Canada, Abstract book, p. 47.

Rampino, M. R., Ernstson, K., Anguita, F., Claudín, F., Pope, K.O., Ocampo,A., and Fischer, A. G., 1997b. Surface features of clasts from impact-ejecta deposits and the "tillite problem". *Abstracts with Prog., Geol. Soc. Am.*, **29**: A-27.

Reiff, W. 1978. Monomict movement breccias; an indicator of meteorite impact. *Meteoritics*, **13**: 605-609.

Robertson, P.B., Dence, M. R. and Vos, M. A 1968. Deformation in rock-forming minerals from Canadian craters. In: French, B. M. and Short, N. M. (eds.), *Shock Metamorphism of Natural Materials*. Mono Book Corp., Baltimore, 433-452.

Roddy, D. J. and Davis, L. K. 1977. Shatter cones formed in large-scale experimental explosion craters. In: *Impact and Explosion Cratering* (D.J. Roddy, R.O. Pepin, R.B. Merrill, eds.), Pergamon Press, New York, 715-750S.

Rösch, C., Hock, R., Schüssler, U., Yule, P. and Hannibal, A. 1997. Electron microprobe analysis and X-ray diffraction methods in archaeometry: Investigations on ancient beads from the Sultanate of Oman and from Sri Lanka. *Eur. J. Mineral.*, **9**: 763-783.

Rust, B.R. 1979. Facies models 2- coarse alluvial deposits. In: G. Walker (ed.): *Facies models*. Geosciencia Canada Reprint Series **1**: 9-21.

Sáez, A. 1985. Upper Eocene-Lower Oligocene terminal fan deposits. Easthern part of the Ebro basin (Suria-Cardona, Spain). *IAS, 6th European Regional Meeting,* Lleida. Abstracts, 854-867.

Saggy, A., Reches, Z. and Fineberg, J. 2002. Dynamic fracture by large extraterrestrial impacts as the origin of shatter cones. *Nature*, **418**: 310-313.

Schwarzmann, E. C., Meyer, C. E. and Wilshire, H. G. 1983. Pseudotachylite from the Vredefort ring, South Africa, and the origins of some lunar breccias. *Bull. Geol. Soc. Amer.*, **94**: 926-935.

Siegert, I. 1997. *Mikrothermometrische und petrographische Untersuchungen an Quarziten der Azuara-Rubielos de la Cérida-Doppelstruktur (Spanien).* Diploma thesis, 72 pp., Universität Bremen.

Spray, J. G. 1997. Superfaults. *Geology*, **25**: 305-308

Stel, H., Rondeel, H. and Smit, J. 2002. Cratered cobbles in Triassic Buntsandstein conglomerates in northeastern Spain: An indicator of shock deformation in the vicinity of large impacts: Comment. *Geology*, **30**: 1052.

Stöffler, D. 1972. Deformation and transformation of rock-forming minerals by natural and experimental shock processes, I. Behavior of minerals under shock compression. *Fortschr. Mineral.*, **49**: 50-113.

Stöffler, D. 1984. Glasses formed by hypervelocity impact. *J. Non-Crystalline Solids*, **67**: 465-502.

Stöffler, D. and Hornemann, U. 1972. Quartz and feldspar glasses produced by natural and experimental shock pressures. *Meteoritics*, **7**: 371-394.

Stöffler, D. and Langenhorst, F. 1994. Shock metamorphism of quartz in nature and experiment: I. Basic observation and theory. *Meteoritics,* **29**, 155 – 181.

Turnbridge, I.P. 1981. Sandy high-energy flood sedimentation - some criteria for recognition, with an example from the Devonian of S.W. England. *Sedim. Geology*, **28**: 79-95

Waasmaier, E. (1988): *Geologische Untersuchungen am S-Rand der Azuara-Struktur (NE-Spanien). Erläuterungen zu einer Kartierung (1 : 10.000) im Gebiet westlich Blesa unter besonderer Berücksichtigung struktureller Merkmale.* Diploma thesis, 108 pp., Universität Würzburg.

Wilson, M. 1989. *Igneous Petrogenesis*. Unwin Hyman, London, 466 pp.

Wilson, C. W. Jr. and Stearns, R. G. 1968. Geology of the Wells Creek Structure, Tennessee. *Tenn. Div. Geol. Bull.*, **68**: 236.

Wilshire, H. G., Offield, T.W., Howard, K. A. and Cummings, D. 1972. *Geology of the Sierra Madera cryptoexplosion structure, Pecos County, Texas*. Geol. Survey Pro. Paper, 599-H, 42 pp.

Wimmenauer, W. 1984. Das prävariskische Kristallin im Schwarzwald. *Fortschr. Mineral. Beih.*, **62**: 69-86.

wt.%	white	white	white	white	white	white	mean
SiO_2	59,95	59,72	59,38	57,19	59,95	59,18	**59,23**
TiO_2	0,24	0,24	0,21	0,20	0,23	0,20	**0,22**
Al_2O_3	20,75	19,53	19,88	21,30	23,16	18,63	**20,54**
MgO	7,26	7,49	7,42	6,14	6,45	8,21	**7,16**
CaO	0,88	1,04	0,92	0,99	1,09	1,17	**1,02**
FeO	1,61	1,77	1,62	1,89	1,85	1,73	**1,75**
Na_2O	1,92	1,87	1,82	1,63	1,56	1,66	**1,74**
K_2O	0,23	0,28	0,27	0,21	0,18	0,26	**0,24**
Total	92,84	91,94	91,52	89,55	94,47	91,04	**91,89**
wt.%	grey	grey	grey	grey	grey		mean
SiO_2	56,45	56,89	58,05	59,54	57,12		**57,61**
TiO_2	0,27	0,21	0,26	0,22	0,25		**0,24**
Al_2O_3	20,81	19,88	19,66	15,99	22,74		**19,82**
MgO	6,77	6,34	7,18	6,90	5,93		**6,62**
CaO	1,14	1,17	1,23	1,24	1,14		**1,18**
FeO	1,68	2,18	1,63	1,51	1,79		**1,76**
Na_2O	1,42	1,19	1,49	0,79	1,31		**1,24**
K_2O	0,21	0,28	0,24	0,23	0,19		**0,23**
Total	88,75	88,14	89,74	86,42	90,47		**88,70**

wt.%	bulk-1	bulk-2	bulk-3	bulk-4	bulk-5
SiO_2	56,06	58,13	53,45	54,47	19,78
TiO_2	0,33	0,34	0,38	0,45	0,24
Al_2O_3	20,91	19,76	20,40	20,96	6,34
MgO	5,81	4,77	5,24	6,14	12,62
CaO	1,48	1,56	1,72	0,98	22,56
FeO	2,00	2,70	2,76	2,49	2,68
Na_2O	0,48	1,20	0,29	0,48	0,02
K_2O	0,65	1,34	0,45	0,57	1,82
LOI	10,30	9,24	14,02	11,70	32,91
Total	98,02	99,04	98,71	98,24	98,97
ppm					
V	14	21	27	23	
Zn	36	46	68	81	
Ga	35	38	30	33	
Rb	16	38	5	7	
Sr	492	363	327	364	
Y	43	37	32	38	
Zr	493	475	491	522	
Nb	56	50	47	53	
Ba	1250	171	48	1034	
Pb	79	238	29	31	
Th	68	59	64	59	

Table 1. Electron microprobe analyses of white and grey glass particles separated from the silicate glass (Pl. 4, Fig.3), and mean compositions. X-ray fluorescence bulk analyses of four samples of the silicate glass (bulk-1 to bulk-4) and one melt-containing inclusion of the suevite (bulk-5

Tabla 1. Analisis con microsonda electrónica de las partículas de vidrio de color blanco-verdoso obtenidas por separación a partir del vidrio silicatado (Pl. 4, Fig.3), en el que se muestra la composición principal. Análisis por fluorescencia de rayos X del preparado de cuatro muestras de vidrio silicatado (preparado-1 a preparado-4) y de un fragmento de fundido que contiene una inclusión procedente de la suevita (preparado-5)

wt.%	1	2	3	4	5	6	mean	bulk
P_2O_5	22,13	21,26	24,47	27,52	32,61	32,42	26,74	8,25
Al_2O_3	0,00	0,00	0,00	0,00	0,00	0,00	0,00	0,00
CaO	35,83	35,97	37,46	42,93	48,76	51,62	42,10	52,65
BaO	0,00	0,00	0,00	0,00	0,00	0,00	0,00	1,47
Na_2O	0,35	0,32	0,46	0,57	0,53	0,55	0,46	0,23
SO_3	1,67	1,15	1,77	2,12	1,47	1,37	1,59	0,92
F	1,57	1,56	1,02	2,26	2,24	2,39	1,84	n.d.
Cl	0,62	0,71	0,50	0,79	0,49	0,55	0,61	n.d.
LOI								34,31
Total	62,18	60,98	65,68	76,19	86,10	88,91	73,34	97,83

Table 2. Electron microprobe analyses of the glassy phosphate matrix (dark areas in Pl. 4, Fig. 7), mean composition of this matrix, and x-ray fluorescence measured bulk composition of the carbonate-phosphate melt

Tabla 2. Analísis mediante microsonda electrónica de la matriz vítrea fosfatada (áreas de color oscuro en la lámina 4, Fig. 7.), mostrando la principal composición de esta matriz, y fluorescencia de rayos X donde se indica la composición global del fundido de cabonato-fosfato.

Plate 1. Breccias from the Azuara impact structure.
Lámina 1. Brechas procedentes de la estructura de impacto de Azuara.

Fig.1. Basal (suevite) breccia. El Portillo variety. Location: UTM coordinates 6 70 500, 45 74 700. The field is 17 cm wide.
Fig.1. Brecha basal (suevita). Variedad el portillo. Localización: coordenadas UTM 6 70 500, 45 74 700. La anchura de campo es de 17 cm.

Fig.2. H-type breccia dike cutting through strongly brecciated limestones. Near Rudilla; UTM coordinates 666660, 4540625.
Fig.2. Dique de brechas del tipo H que atraviesa calizas fuertemente brechadas. Cerca de Rudilla; coordenadas UTM 666660, 4540625

Fig.3. Schocked polymictic breccia from a dike cutting through Palaeozoic rocks near Santa Cruz de Nogueras. Note the fitting of the components proving immediate cementation after the brecciation. Location: UTM coordinates 661240, 4553400. The field is 23 cm wide.
Fig. 3. Brecha polimíctica chocada que proviene de un dique, sito cerca de Santa Cruz de Nogueras, que atraviesa rocas del Paleozoico. Observese el encaje de los componentes de la misma que prueba una inmediata cementación después de la brechificación. Localización: coordenadas UTM 661240, 4553400. La anchura del campo es de 23 cm.

Fig.4. Impact breccia from Almonacid de la Cuba (see tex). The field is 16 cm wide.
Fig. 4. Brecha de impacto procedente de Almonacid de la Cuba (ver el texto). La anchura de campo es de 16 cm.

Fig.5. Megaclasts from the megabreccia; old railway cut near Belchite, UTM coordinates 689450, 4569350. Note that the left block is completely converted into a grit breccia.
Fig. 5. Megaclastos sitos en la megabrecha; corte de la antigua via de tren cercano a Belchite; coordenadas UTM 689450, 4569350. Puede apreciarse como el bloque situado a la izquierda esta completamente transformado en una brecha arenosa.

Fig.6. Monomictic movement breccia; near Monforte de Moyuela, UTM coordinates 667050, 4547030. The field is 20 cm wide.
Fig. 6. Brecha de movimiento monomíctica situada cerca de Monforte de Moyuela; coordenadas UTM 667050, 4547030. La anchura de campo es de 20 cm.

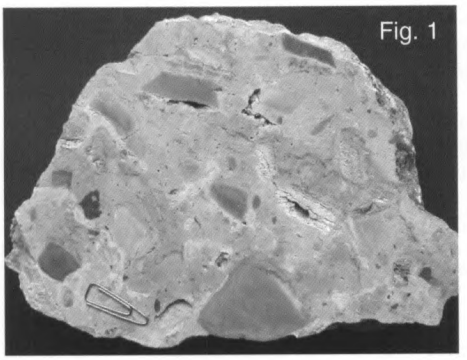
Fig. 1

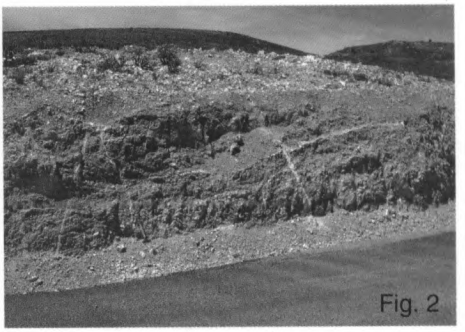
Fig. 2

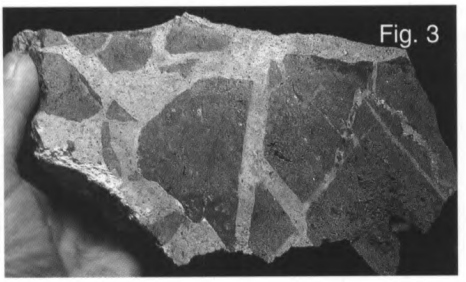
Fig. 3

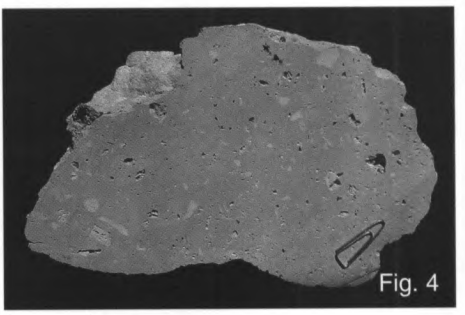
Fig. 4


Fig. 5

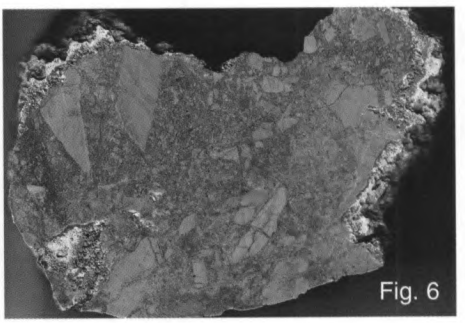
Fig. 6

Plate 2. Shock metamorphism in rocks from the Azuara (Fig.1-6) and Rubielos de la Cérida (Fig.7, 8) impact structures.
Lámina 2. Metamorfismo de choque presente en las rocas de las estructuras de impacto de Azuara (Fig. 1-6) y Rubielos de la Cérida (Fig. 7, 8).

Fig.1. Melt glass with vesicles, schlieren and mineral fragments; photomicrograph, plane polarized light and crossed nicols. Strongly shocked dike breccia, near Santa Cruz de Nogueras. The field is 9 mm wide.
Fig.1. Vidrio fundido con vesículas, bandas y fragmentos minerales; microfotografia realizada a luz paralela y a nícoles cruzados. Dique de brechas fuertemente chocado cercano a Santa Cruz de Nogueras. La anchura de campo es de 9 mm.

Fig.2. Diaplectic glass; photomicrograph of a sandstone fragment completely transformed to diaplectic quartz; plane polarized light and crossed nicols. The fragment is embedded in partly recrystallized melt glass. Note that there are a few holes in the thin section not to be confused with diaplectic quartz grains. Strongly shocked dike breccia, near Santa Cruz de Nogueras. The field is 600 μm wide.
Fig.2. Vidrio diapléctico; microfotografia realizada a luz paralela y a nícoles cruzados, de un fragmento de arenisca completamente transformado en cuarzo diapléctico. El fragmento se halla inmerso en el seno de un fundido vítreo parcialemente recristalizado. Puede apreciarse la presencia de algunos agujeros en la sección delgada que no deben ser confundidos con granos de cuarzo diaplécticos. Dique de brechas fuertemente chocado cercano a Santa Cruz de Nogueras. La anchura de campo es de 600 μm.

Fig.3. Partly isotropic quartz grain (diaplectic crystal); monomictic dike breccia, S Ventas de Muniesa, UTM coordinates 687980, 4552360 (Mayer 1990). Photomicrograph, crossed nicols; the field is 195 μm wide.
Fig. 3. Grano de cuarzo parcilmente isotrópico (cristal diapléctico); dique de brechas monomícticas situado al S de Ventas de Muniesa; coordenadas UTM 687980, 4552360 (Mayer, 1990). Microfotografia realizada a nícoles cruzados; la anchura de campo es de 195 μm.

Fig.4. Multiple sets of planar deformation features (PDFs) in quartz; strongly shocked polymictic dike breccia, Santa Cruz de Nogueras. At least six sets of decorated PDFs can be observed. Photomicrograph, crossed nicols; the field is 140 μm wide.
Fig.4. Múltiples conjuntos de rasgos de deformación planar (PDFs) en un cuarzo; dique de brechas fuertemente chocado sito cerca de Santa Cruz de Nogueras. Al menos pueden ser observados seis conjuntos de PDFs decoradas. Microfotagrafia realizada a nícoles cruzados; la anchura de campo es de 140 μm

Fig.5. Multiple sets of planar fractures (PFs; cleavage) in quartz; autochthonous Utrillas sandstone near Blesa (Waasmaier 1988). Six different PF orientations can be observed. Photomicrograph, crossed nicols; the field is 80 μm wide.
Fig.5. Múltiples conjuntos de fracturas planares (PFs; clivaje) presentes en cuarzos; arenisca autóctona de la Fm. Utrillas cercana a Blesa (Waasmaier, 1988). Pueden observarse seis diferentes orientaciones de PF. Microfotografia obtenida a nícoles cruzados; la anchura de campo es de 80 μm.

Fig.6. Microtwinning and kinkband in calcite; polymictic dike breccia, N Muniesa, UTM coordinates 685380, 4547630 (mayer 1990). Photomicrograph, crossed nicols; the field is 150 μm wide.
Fig. 6. Micromaclado y bandas de kink en calcita; dique de brechas polimíctico sito al N de Muniesa; coordenadas UTM 685380, 4547630 (Mayer, 1990). Microfotografia realizada a nícoles cruzados; la anchura de campo es de 150 μm.

Fig.7. Diaplectic feldspar crystal with isotropic spots and one set of isotropic twinning lamellae, typical of shock metamorphism; silicate melt rock, Rubielos de la Cérida structure. Crossed polarizers; the field is 1 mm wide.
Fig.7. Cristal de feldespato diapléctico con agujeros isotrópicos y con un conjunto isotrópico de bandas de maclado, típico de metamorfismo de choque; roca de fundido silicatado de Rubielos de la Cérida. Microfotografia realizada a nícoles cruzados; la anchura de campo es de 1 mm.

Fig.8. Disintegrated feldspar showing strong mechanical twinning and multiple sets of planar deformation features (PDF). Clast from the Barrachina megabreccia, Rubielos de la Cérida structure. Crossed polarizers; the field is about 900 μm wide.
Fig.8. Feldespato desintegrado que muestra un intenso maclado mecánico y mútiples conjuntos de estructuras de deformación planar (PDFs). Clasto procedente de la megabrecha de Barrachina, ubicada en la estructura de impacto de Rubielos de la Cérida. Microfotografia obtenida a nicoles cruzados; la anchura de campo es de 900 μm.

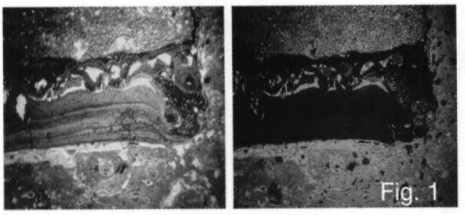
Fig. 1

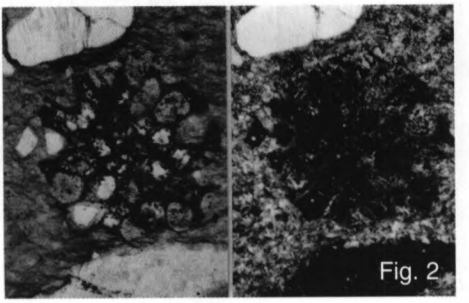
Fig. 2

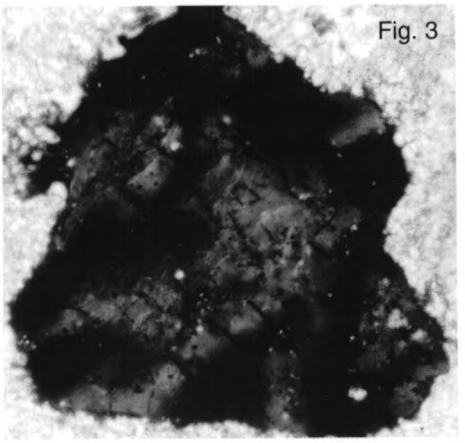
Fig. 3

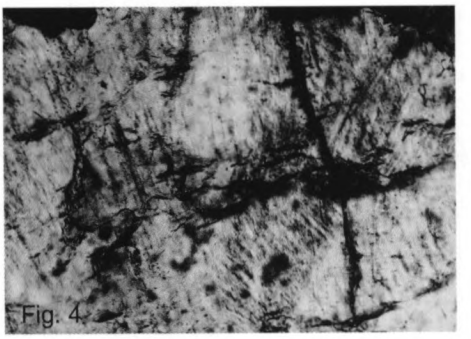
Fig. 4

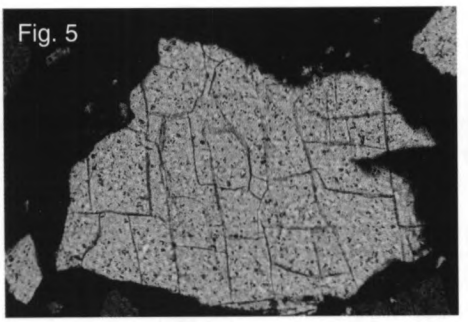
Fig. 5

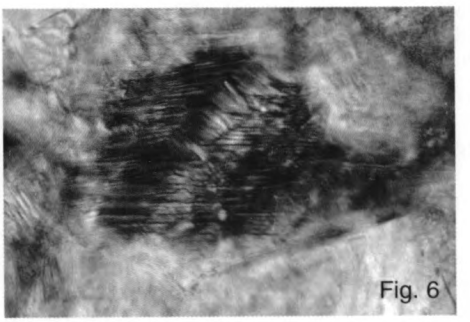
Fig. 6

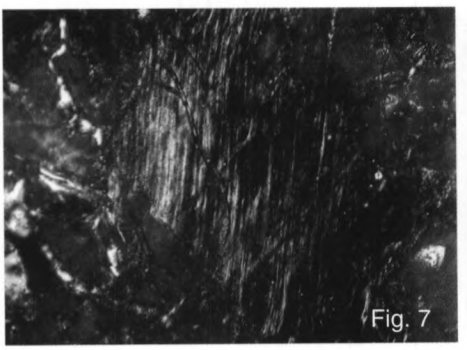
Fig. 7

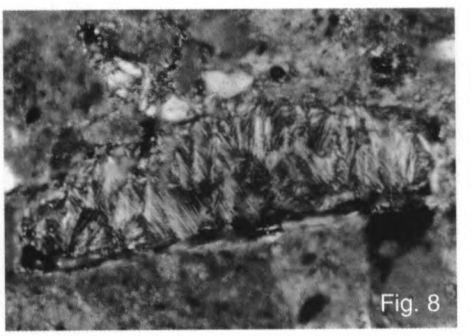
Fig. 8

Plate 3. Rubielos de la Cérida impact structure: Breccias and breccia dikes.
Lámina 3. Estructura de impacto de Rubielos de la Cérida: brechas y diques de brechas.

Fig.1, Fig.2. Megabrecciation of Jurassic limestones in the southern central uplift. Note the chaotic criss-cross layering (2) and some "ghost" layering having survived the intense brecciation (1). UTM coordinates 643310, 4510560 (1); 646100, 4508000 (Bueña village) (2).
Fig.1., Fig.2. Megabrechificación en calizas del Jurásico ubicadas en la parte sur del levantamiento central. Puede apreciarse la estratificación caótica entrelazada (2) y alguna estratificación relicta que ha podido sobrevivir a la intensa brechiación (1). Coordenadas UTM 643310, 4510560 (1); 646100, 4508000 (pueblo de Bueña) (2).

Fig.3. Polymictic breccia dike cutting through competent Muschelkalk limestones. Near Olalla, UTM coordinates 657750, 4537800
Fig. 3. Dique de brechas polimícticas que atraviesa calizas competentes del Muschelkalk. Cerca de Olalla; coordenadas UTM 657750, 4537800.

Fig.4. Dike cutting through Jurassic limestones near Ojos Negros; UTM coordinates 626100, 4510900 The white material is assumed to be crystallized carbonate melt.
Fig.4. Dique que atraviesa calizas del Jurásico cercanas a Ojos Negros; coordenadas UTM 626100, 4510900. El material blanquecino corresponde a fundido carbonatado cristalizado.

Fig.5. Megabreccia near Barrachina (UTM coordinates6 55 100, 45 29 900) showing three megaclasts of different lithology in contact. A microbreccia (whitish colour) seems to have been injected into the middle, diamictic clast.
Fig.5. Megabrecha cercana a Barrachina (coordenadas UTM 655100, 4529900) donde se pueden apreciar 3 megaclastos en contacto de diferente litologia. Una microbrecha (de color blanquecino) parece haber sido inyectada en la parte media del clasto diamíctico.

Fig.6. Multicoloured breccia as part of the megabreccia near Barrachina: an intense mixture of diamictic, mostly Palaeozoic material and ?Lower Tertiary red and green marls (darker clasts). Temporary quarry (now filled up) at the bank of the Pancrudo brook.
Fig.6. Brecha multicolor que forma parte de la megabrecha cercana a Barrachina: una mezcla intensa de materiales diamícticos, en su mayoría del Paleozoico y de margas rojo verdosas del Terciario inferior (¿?) (clastos mas oscuros). Cantera temporal (ahora rellenada) situada en la orilla del arroyo de Pancrudo.

Fig.7. Megabreccia near Barrachina: grit-brecciated limestone megaclast partly interspersed with a marly to sandy matrix. A few larger clasts have survived the heavy brecciation, and some preserved ghost-layering is observed. UTM coordinates 6 52 310, 45 30 950.
Fig.7. Megabrecha cercana a Barrachina: megaclasto calizo intensamente brechificado (hasta tamaño arena) parcialmente entremezclado con una matriz arenoso-margosa. Unos pocos clastos de gran tamaño han sobrevivido a la intensa brechificación. De igual modo, puede apreciarse alguna estratificación relicta. Coordenadas UTM 6 52 310, 45 30 950.


Fig. 1

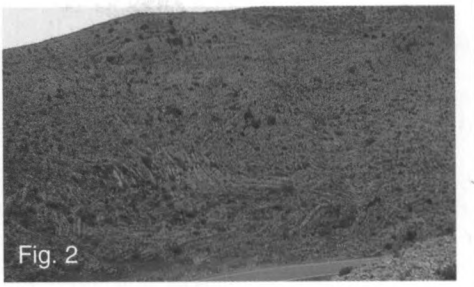
Fig. 2


Fig. 3


Fig. 4


Fig. 5


Fig. 6

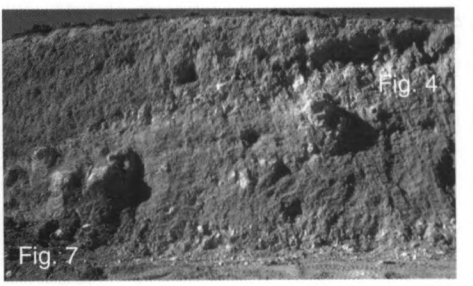
Fig. 7

Plate 4. Melt rocks in the Rubielos de la Cérida structure.
Lámina 4. Rocas fundidas en la estructura de impacto de Rubielos de la Cérida.

Fig.1, Fig.2: Megabreccia near Barrachina: Typically intercalated silicate melt rocks (the whitish ribbons and clasts).
Fig.1, Fig. 2: Megabrecha cercana a Barrachina: Rocas de fundido silicatado típicamente intercaladas (los clastos y cintas blanquecinos)

Fig.3. The silicate melt rock under the microscope. The rock is composed of estimated more than 90 % glass forming tiny spheroids and lens-shaped bodies. The field is about 8 mm wide.
Fig.3. Aspecto de la roca de fundido silicatado bajo el microscopio. La roca esta compuesta por más de un 90% de vidrio bajo la forma de delgadas esférulas y cuerpos con forma de lentejón. La anchura de campo es de 8 mm.

Fig.4. Sawed surface of a suevite sample from a large block quarried out from the Barrachina megabreccia.
Fig.4. Superfície cortada de una muestra de suevita procedente de un gran bloque extraido de la megabrecha de Barrachina.

Fig.5. Suevite-like dike breccia intercalated in strongly brecciated limestones.
Fig.5. Dique de brecha del tipo suevítico intercalado en calizas intensamente brechadas.

Fig.6. Clast of carbonate-phosphate melt rock (white) in the Barrachina megabreccia. Coin diameter 23 mm.
Fig.6. Clasto de roca de fundido carbonatado-fosfatado (color blanquecino) presente en la megabrecha de Barrachina. El diámetro de la moneda es de 23 mm.

Fig.7. Photomicrograph (crossed polarizers) of amoebae-like calcite bodies within a matrix of phosphate glass (dark) from the clast in Fig.6. Note that the size of the individual calcite crystals increases towards the centers of the bodies. Also note that the peripheral calcite obviously has grown perpendicular to the rim because of the orientation. In part, especially along the borders to the calcite bodies, the phosphate glass has recrystallized to form apatite (elongated, sometimes flaser-like minerals tangentially orientated to the calcite bodies). The field is 6 mm high.
Fig.7. Microfotografia (a nícoles cruzados) de cuerpos de calcita ameboidales sitos dentro de una matriz de vidrio fosfatado (color oscuro), obtenida a partir del clasto de la Fig. 6. Puede observarse que el tamaño de los cristales individuales de calcita aumenta hacia el centro de los cuerpos. También puede apreciarse que la calcita de la periferia ha crecido obviamente de modo perpendicular al borde a causa de la orientación. En parte, y especialmente a lo largo de los bordes de los cuerpos de calcita, el vidrio fosfatado ha recristalizado para formar apatito (en minerales de formas elongadas, a veces con formas filamentosas, orientados tangencialmente respecto a los cuerpos de calcita). La anchura de campo es de 6 mm.

Fig.8. Microslag-like particles are common in blocks of a finegrained microbreccia within the Barrachina megabreccia. They consist of amorphous carbon with subordinate amounts of Ca and S, but also contain remarkable amounts of oxygen. Scale bar is 1 mm.
Fig.8. Partículas de morfologia similar a la microescoria son comunes en bloques de una microbrecha de grano fino sita dentro de la megabrecha de Barrachina. Estas partículas consisten en carbón amorfo con cantidades subordinadas de Ca y S, pero también contienen cantidades remarcables de oxígeno. La escala de la barra es de 1 mm.

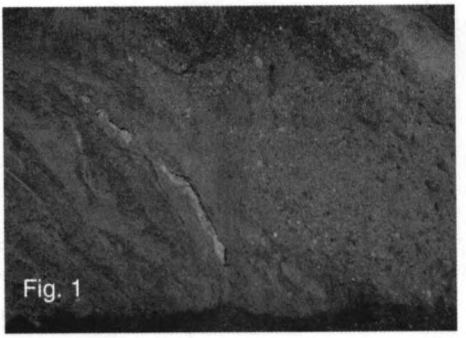
Fig. 1

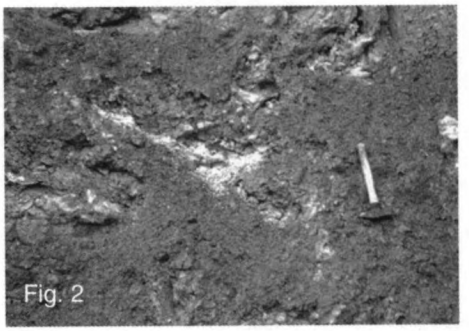
Fig. 2


Fig. 3

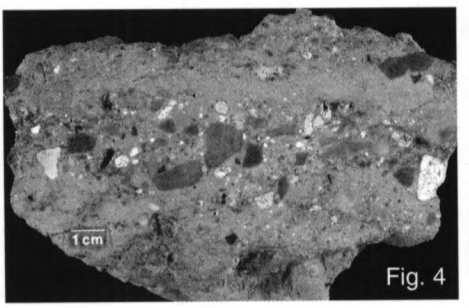

Fig. 4


Fig. 5

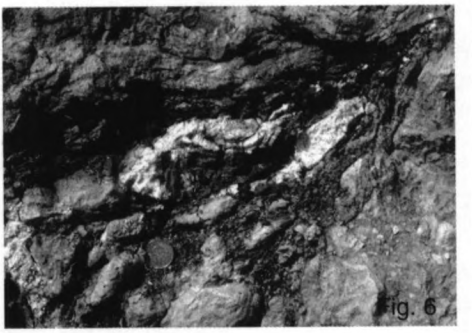
Fig. 6

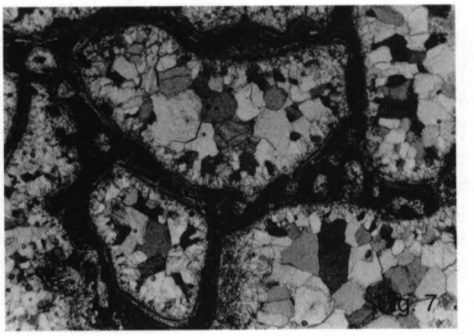
Fig. 7

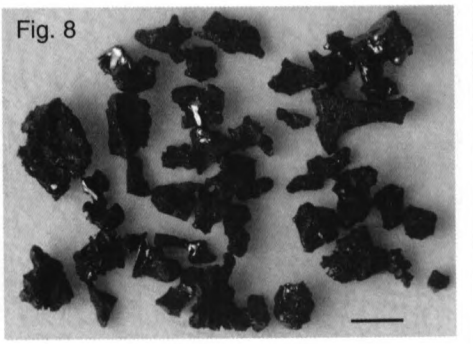
Fig. 8

Plate 5. Pelarda Fm. and Puerto Mínguez impact ejecta.
Lámina 5. Eyectas de la Fm. Pelarda y de Puerto Mínguez.

Fig.1. Typical aspect of the middle unit of the Pelarda Fm. showing matrix-supported texture.
Fig.1. Aspecto típico de la unidad media de la Fm. Pelarda en el que exhibe una textura soportada por la matriz.

Fig.2. Strongly deformed quartzite clast from the Pelarda Fm. ejecta; near Olalla, UTM coordinates 655700, 4537250. Despite the remarkable displacements, the clast remains coherent and is not broken into pieces.
Fig.2. Clasto de cuarcita intensamente deformado procedente de los yecta de la Fm. Pelarda; cerca de Olalla, coordenadas UTM 655700, 4537250. A pesar de los evidentes desplazamientos, el clasto permanece unido y no se halla roto en fragmentos.

Fig.3. Multiple sets of striae on a quartzite cobble. The field is 2.5 cm wide.
Fig.3. Múltiples conjuntos de estrias sobre un canto de cuarcita. La anchura del campo es de 2,5 cm.

Fig.4. SEM image of two sets of crossing PDFs in quartz; shocked Bámbola quartzite clast from the Pelarda Fm. ejecta. Note the spacing of the individual PDFs, which is distinctly less than 1 μm in many cases.
Fig.4. Imagen SEM de dos conjuntos de PDFs que se intersectan en un cuarzo; clasto chocado de cuarcita Bambolar procedente del eyecta de la Fm. Pelarda. Observese el espaciado de las PDFs individuales, que es típicamente inferior a 1 μm en algunos casos.

Fig.5. Typical aspect of the Puerto Mínguez ejecta. The outcrop height is about 12 m.
Fig.5. Aspecto típico del eyecta de Puerto Mínguez. La altura del afloramiento es de 12 m.

Fig.6. Puerto Mínguez impact ejecta: Mesozoic limestone cobbles and boulders in dominating Palaeozoic matrix material. The outcrop height is about 6 m.
Fig. 6. Eyecta de impacto de Puerto Mínguez: cantos y bloques de calizas del Mesozoico dentro de una matriz dominante de materiales del Paleozoico. La altura del afloramiento es de 6 m.

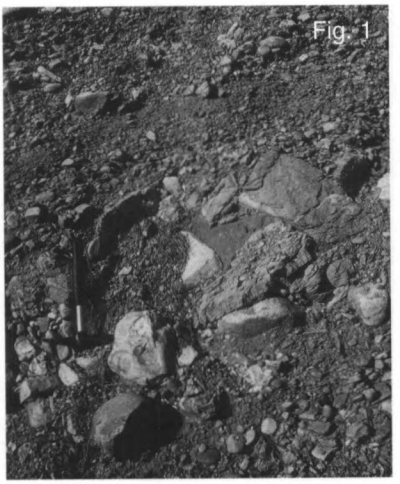
Fig. 1


Fig. 2

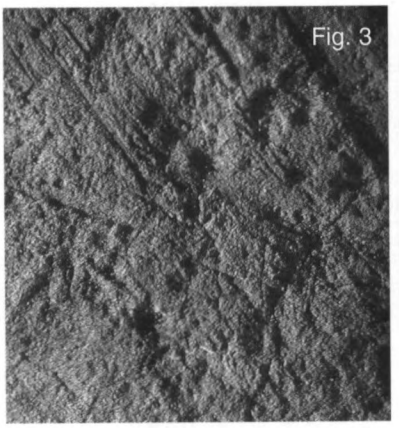
Fig. 3

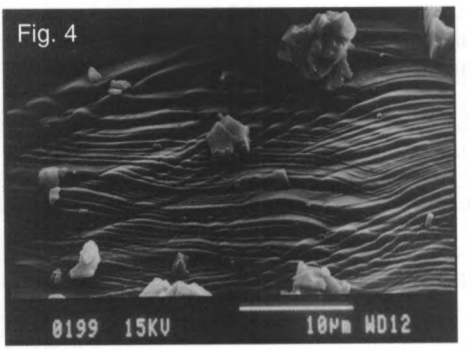

Fig. 4


Fig. 5


Fig. 6

Plate 6. Puerto Mínguez impact ejecta and shock-deformed Buntsandstein cobbles.
Lámina 6. Eyecta de impacto de Puerto Mínguez y cantos deformados por impacto del Buntsandstein.

Fig.1. Breccia zone in the Puerto Mínguez diamictite. Hammer length is 40 cm.
Fig.1. Zona de brecha en la diamictita de Puerto Mínguez. La longitud del martillo es de 40 cm.

Fig.2. Striated surface of a limestone boulder. Centimeter scale.
Fig. 2. Superfície estriada de un bloque calizo. Escala centimétrica.

Fig.3. Fine striation of a limestone boulder merging into mirror polish. Centimeter scale.
Fig.3. Estriación fina en un bloque calizo que se halla en una zona de pulido en espejo. Escala centimétrica.

Fig.4. Penetration marks in strongly deformed limestone cobbles from the Puerto Mínguez ejecta. Centimeter scale.
Fig.4. Marcas de penetración presentes en cantos calizos intensamente deformados procedentes del eyecta de Puerto Mínguez. Escala centimétrica.

Fig.5. Limestone cobbles from the Puerto Mínguez ejecta showing internal rotations with macroscopically untouched hinges (arrows) and rotated fractures. Note the two axes of rotation in the cobble down to the right. Centimeter scale.
Fig.5. Cantos calizos procedentes del eyecta de Puerto Mínguez que exhiben rotaciones internas con charnelas macroscópicas no deformadas (flechas) y fracturas rotacionales. Apréciense los dos ejes de rotación en el canto hacia la parte inferior derecha. Escala centimetrica.

Fig.6. "Bread cut to slices" type of deformation in limestone cobble from the Puerto Mínguezejecta. Note that the cobble is not broken into pieces.
Fig.6. Deformación del tipo "rodajas de pan" presente en un canto calizo procedente del eyecta de Puerto Mínguez. Puede observarse como el canto no se encuentra roto en fragmentos.

Fig.7. Typically shock-deformed quartzite cobble from autochthonous Buntsandstein basal conglomerates; deposits between Rueda de la Sierra and Molina de Aragón. Length of cobble 17 cm. The pockmarks have originated from fracturing upon collision with neighbouring cobbles and lack any dissolution features.
Fig.7. Canto de cuarcita, tipicamente deformado por choque, procedente de los conglomerados autóctonos del Buntsandstein basal; depósito localizado entre Rueda de la Sierra y Molina de Aragón. La longitud del canto es de 17 cm. Los hoyos se han originado a partir de la fracturación por el choque con los cantos vecinos, no presentando ningún rasgo de disolución.

Fig.8. Cratered quartzite cobble from autochthonous Buntsandstein basal conglomerates; deposits between Rueda de la Sierra and Molina de Aragón. Maximum size of cobble 6 cm. The crater proves brittle fracturing and has probably formed by spallation from shock collision.
Fig.8. Canto de cuarcita con cráteres procedente de los conglomerados autóctonos del Buntsandstein basal; depósito localizado entre Rueda de la Sierra y Molina de Aragón. El tamaño máximo del canto es de 6 cm. El cráter es una prueba de fracturación frágil y se ha formado probablemente por espalación a partir de la colisión.

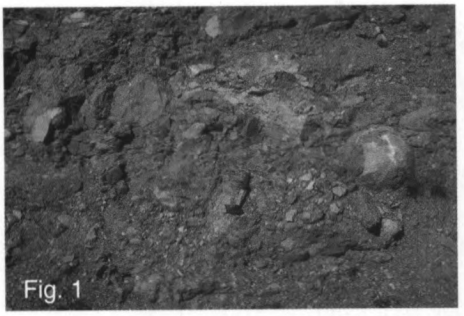
Fig. 1

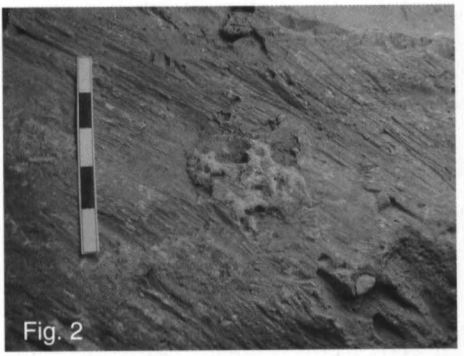
Fig. 2

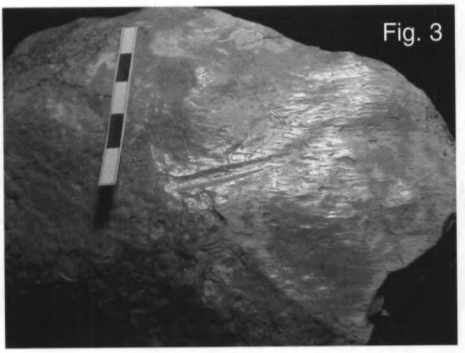
Fig. 3


Fig. 7

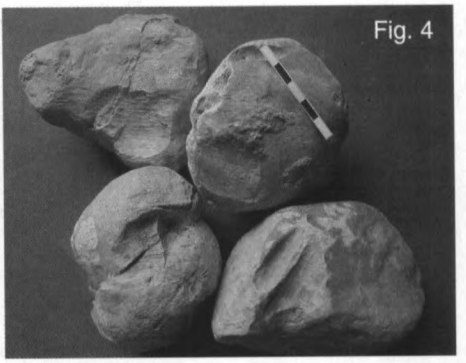
Fig. 4

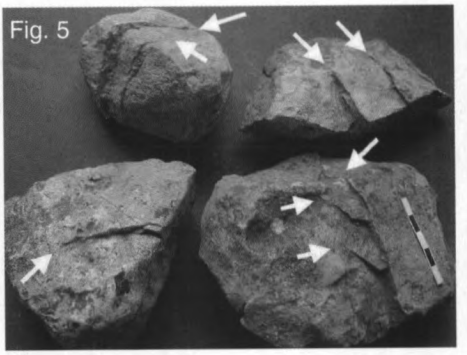
Fig. 5


Fig. 6

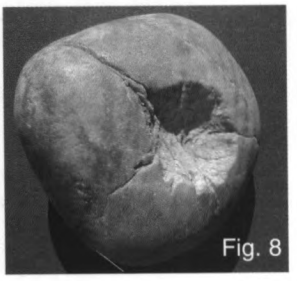
Fig. 8